METEOROLOGICAL OFFICE RADAR RESEARCH LABORATORY

RSRE MALVERN ENGLAND

RESEARCH REPORT

No. 15

December 1979

PERMISSION TO QUOTE FROM THIS INTERNAL REPORT MUST BE OBTAINED FROM THE CHIEF MET. OFFICER

Radar Observations of the Troposphere in Clear Air Conditions

P K JAMES

Meteorological Office Radar Research Laboratory

RSRE

St Andrews Road,

Malvern, Worcs.

ABSTRACT

It is now 15 years since radars were first used intensively to probe the atmosphere in clear air conditions. The first experiments were concerned with the nature of the targets and accounting for the intensity of the measured echoes. It was found that inhomogeneities in the refractive index field were responsible for a large proportion of clear air returns. Such returns were detected in characteristic patterns in association with sheared statically stable layers, convective thermals, air mass boundaries and a variety of wave structures. More sensitive Doppler radars have been developed in recent years which are able to obtain usable signals from all heights in the troposphere. Such radars, as well as providing additional information about the clear air patterns observed previously, enable continuous measurements of wind profiles to be made. This paper describes the phenomena which have been observed and the measurements which have been made with radars under clear air conditions. A summary is given of the types of targets observed and the kinds of radars used in clear air studies are briefly described.

1. INTRODUCTION

Early observations of radar returns which could not be attributed to aircraft or precipitation were referred to as 'angels' (Atlas, 1964) and much speculation surrounded the possible origins of these mysterious targets. However by the time Hardy and Katz (1969) wrote their review article on clear-air radar echoes it became clear that two types of target were responsible for the returns: (i) discrete targets such as insects and birds and (ii) extended targets, mainly refractive index inhomogeneities but under some special circumstances specular reflection from layered structures in the refractive index field. Important events in the period when the nature of the returns was being investigated include the observation of stable layers (Lane and Meadows, 1963), of the tropopause (Atlas et al., 1966a), of insects and birds (Glover and Hardy, 1966), and of clear air convection (Hardy and Ottersten, 1969), multiwavelength measurements of extended and point targets (Hardy et al., 1966) and the observation of a layer having the appearance of a braided rope (Hicks and Angell, 1968). This last observation proved to be especially stimulating as it was found that the air motions responsible for the production of such characteristic returns also caused clear air turbulence. All these observations were basically of patterns and signal intensities and were all made with pulsed non-Doppler radars. Progress to the end of the 1960s has been summarized by Hardy (1972), Ottersten (1969a) and Battan (1973).

Around 1970 two instrumental advances were made: highly sensitive pulsed Doppler radars (Dobson, 1970; Browning et al., 1972) and high resolution (although non-Doppler) FM-CW radars (Richter, 1969) became available. Observations with FM-CW radars revealed in detail wave motions in the boundary layer with amplitudes as small as a few metres (Ottersten et al., 1973; Richter et al.,1973a). Doppler processing has since been added to FM-CW radars making them a potent tool for boundary layer investigations (Chadwick et al.,1976) Pulsed Doppler radars have developed throughout the 1970s to the stage that a dual Doppler system has been constructed which is able to sense two components of the wind in the boundary layer over a 25 x 25 km area (Doviak and Jobson, 1979). Other pulsed Doppler radars have been developed capable of obtaining continuous wind soundings throughout the troposphere (Green et al., 1975a). The development and use of such radars has been described by Gage and Balsley (1978).

In Section 2 of this article we consider the types of radar target which allow measurements to be made in the clear air and in Section 3 we describe the various radars used in clear air studies. Section 4 describes phenomena observed with non-Doppler radars and Section 5 the measurements made mainly with Doppler radars. Finally some of the more promising applications of clear air observations are described in Section 6.

2. TYPES OF RADAR TARGET AVAILABLE FOR MEASUREMENTS IN THE OPTICALLY CLEAR AIR

Clear air echoes are generally taken to be echoes received from targets other than precipitation, large cloud drops or ice particles. Since very small cloud particles can give radar reflectivities smaller than 'clear air targets' within the same pulse volume, it is possible to obtain clear air returns in some non-precipitating clouds. The conditions required are more readily realised at longer wavelengths.

2.1 RADAR RETURNS DUE TO INCOHERENT SCATTERING FROM REFRACTIVE INDEX INHOMOGENEITIES

The primary cause of clear air echoes from extended targets is scattering from refractive index inhomogeneities. Scattering occurs only from inhomogeneities on a scale of one half the radar wavelength (Tatarski, 1961), such irregularities being produced from larger scale refractive index gradients by turbulence. The radio refractive index depends mainly on air temperature and water vapour pressure (Bean and Dutton, 1968). In the upper troposphere the water vapour pressure is small and only temperature gradients make a significant contribution to refractive index gradients. In the lower troposphere the refractive index is more sensitive to humidity. Conditions for the production of suitably large inhomogeneities may be found in association with sheared stable layers, air mass boundaries, cloud and fog tops, convective boundaries, the tropopause and thunderstorm gust fronts.

Ottersten (1969b) describes the general relationship between radar reflectivity (η) and refractive index variations. Under certain simplifying conditions (Hardy et al., 1966), the reflectivity is related to C_n^2, the refractive index structure constant, defined as the rms difference in refractive index at two points unit distance apart, by

$$\eta \sim 0.38\, C_n^2\, \lambda^{-\frac{1}{3}} \qquad (1)$$

These conditions are, that the turbulence producing the inhomogeneities should be isotropic and uniformly should fill the radar resolution volume, that one half the radar wavelength must fall within the inertial subrange and that no other targets such as insects, cloud droplets or specular reflection should contribute to the reflectivity.

The limiting microscale of the inertial subrange is of the order of a few millimetres in the planetary boundary layer increasing to a few centimetres in the upper troposphere. On scales smaller than the limiting microscale turbulence and hence refractive index variations are heavily damped by viscous processes, precluding the use of very short wavelengths for clear air observations (Atlas et al.,1966a). The outer scale of the inertial subrange may be as large as several hundred metres in neutral or convective conditions or less than one metre within thin statically stable layers (Metcalf and Atlas, 1973). Thus in the case of stable layers the assumption that turbulence is uniform throughout the pulse volume is questionable as is the assumption that one half the radar wavelength falls within the inertial subrange for metre wavelengths.

Comparisons of C_n^2 measured by radar with in-situ refractometer measurements have been made by Kropfli et al.(1968), Bean et al.(1971) and Konrad and Robison (1972). All used 10 cm radars but their refractometers were insensitive to fluctuations on scales smaller than 20 cm so the in-situ measurements had to be extrapolated to 5 cm (one half the radar wavelength) using a -5/3 spectral law on the assumption of an inertial subrange. The results agreed to within factors of 2 to 4 as C_n^2 changed by two orders of magnitude despite the uncertainties involved in the comparisons.

Values of C_n^2 show considerable variability as a function of time, altitude and horizontal position. Measurements by VanZandt et al.(1978) have shown four-minute averages of C_n^2 obtained at a height of 10 km can change by more than an order of magnitude in a few tens of minutes. Figure 1 shows a vertical profile of C_n^2 averaged over a period of 36 minutes (Ecklund et al., 1977). C_n^2 decreases by more than two orders of magnitude between 2 and 8 km, such a decrease being quite typical. Measurements made around a circle 13 km in diameter at an altitude of 7 km have also shown order of magnitude variations from one part of the circle to another (Gage and Balsley,1978). Figure 2 shows some statistics of C_n^2 obtained during a one year operation at Boulder, Colorado (Chadwick et al.,1978a,b). The observations were made with range and time resolutions of 160 m and 1 minute respectively. The figure shows as a function of time of day the percentage of observations which were less than given values of C_n^2. For instance at midnight only 5% of observed C_n^2 values were less than $8 \times 10^{-17}\ m^{-\frac{2}{3}}$. The lowest observed values were consistently above $10^{-17}\ m^{-\frac{2}{3}}$. Aircraft measurements (Ochs and Lawrence, 1972) have also shown that the contribution of temperature fluctuations alone to C_n^2 is normally greater than $10^{-17} m^{-\frac{2}{3}}$ in the first 3 km of the atmosphere. Although it is possible that the contribution of humidity fluctuations to C_n^2 might partially cancel the temperature contribution it has been suggested that this minimum figure should be used when calculating the desired sensitivity of radars required to continuously sense winds in the boundary layer (Hennington et al.,1976). In contrast values of C_n^2 as large as $10^{-9} m^{-\frac{2}{3}}$ have been measured within thin echo layers with a 1 metre resolution radar (Richter, 1969). For comparison 1 mm h^{-1} of rain observed with a 10 cm wavelength radar would give the same reflectivity as turbulence with C_n^2 equal to $10^{-9} m^{-\frac{2}{3}}$.

Gossard (1977) has calculated the height dependence of C_n^2 in different air mass types and in an air mass being modified at its lower boundary (Gossard, 1978a,b). The calculations show that average values of C_n^2 vary from about $10^{-14} m^{-\frac{2}{3}}$ near the surface to around $10^{-16} m^{-\frac{2}{3}}$ at 5 km height. However the variation of Cn^2 about its average in a given air mass is much greater than the variation of the mean from air mass to air mass so the utility of such calculations awaits more extensive measurements. VanZandt et al. (1978) have attempted to relate the vertical variation of hourly averages of C_n^2 to quantities measurable from radiosonde ascents. One feature of their model is that they allow for the possibility that only a fraction of the measurement volume is turbulent. Although there are a number of assumptions which are difficult to justify, the model results are in reasonable agreement with averaged C_n^2 profiles.

2.2 OTHER KINDS OF CLEAR AIR RADAR RETURNS

a) RADAR RETURNS DUE TO SPECULAR REFLECTIONS FROM REFRACTIVE INDEX GRADIENTS

Partial specular reflection from layered structures in the refractive index field can provide a significant contribution to clear air reflectivity in some circumstances. Such returns appear to be more important for longer wavelength radars operating in the vertical-pointing mode. Thus, for example, examination at 10 cm wavelength of the signal received from an echo layer at 800 m height as a function of angle of incidence has shown no evidence for enhanced reflection at vertical incidence (Richter et al., 1973a). On the other hand measurements made at a wavelength of 5.6 m show considerably enhanced signals from certain layers at vertical incidence. (Röttger, 1978; Röttger and Liu, Röttger and Vincent, 1978). Figure 3 shows time-height observations of reflectivity made at vertical (VE) and oblique (OB) incidence. For some layers at around 3 km height the return signal was 20 db higher in the vertically pointing mode. The signal from such layers proved to have a significant degree of coherence over periods as long as 100 seconds which also suggests a reflection mechanism other than refractive index inhomogeneities which have coherence times of less than a few seconds.

At present theories of specular reflection assume rather idealized reflectivity profiles. Further progress in understanding this type of radar return awaits both more detailed observations and the development of more satisfactory theoretical descriptions of the phenomenon.

b) RADAR RETURNS FROM DISCRETE TARGETS

Discrete targets observed in clear air studies include insects and birds. Radar ornithology (Eastwood,1967) and entomology (Riley,1979) have developed as disciplines in their own right.

Small insects which are generally slow fliers are good tracers of air motion. Some studies have measured the Doppler velocity of insects carried by the wind (eg Lhermittee,1966; Browning and Atlas,1966) whilst others have observed the concentration of insects in regions of convergence such as sea breeze fronts (Geotis,1964), thunderstorm gust fronts (Harper,1958, 1960) or in association with atmospheric layer structures (Richter et al.,1973b). For insects whose size is much smaller than the radar wavelength Rayleigh backscattering applies and the radar cross section is proportional to λ^{-4}, as opposed to $\lambda^{-\frac{1}{3}}$ for refractive index inhomogeneities. Birds and larger insects fly at significant speeds and are unreliable as air motion tracers unless fortutious circumstances - such as the concentration of insect food in a region of convergence - apply (Eastwood,1967).

Chaff is occasionally used to allow radars with modest sensitivites to follow air motion. However, such methods are logistically inconvenient and are restricted to rather limited volumes of the atmosphere.

3. TYPES OF RADARS AND FACTORS AFFECTING THEIR SENSITIVITY

3.1 TYPES OF RADAR

A variety of radars have been developed or modified for clear air studies. Existing systems use pulsed or FM-CW transmitters operating on wavelengths between 3 cm and 7.5 m together with reflecting dishes or phased arrays which may or may not be steerable. Most of the radars recently developed utilise Doppler processing to maximise the information obtained from reflected signals. The characteristics of some of the radar systems used for clear air studies in the last decade are given in Table 1.

In a pulsed radar system the target range is determined by the time between pulse transmission and receipt of the reflected signal. In FM-CW systems the transmitter is operated continuously but its frequency is changed linearly with time, the difference between the frequency of the reflected signal and the current transmitter frequency is a measure of the range of the target. The spatial resolution obtained with a radar depends both on the range resolution and the angular width of the beam. The steerable dishes with pulsed transmitters are generally configured to provide medium range and beamwidth resolution (30 to 300 m) in the lower and middle troposphere. The pulsed phased arrays allow measurements to be made throughout the troposphere albeit at reduced resolution (~ 1 km range resolution, 500 m beamwidth resolution at 10 km range). FM-CW radars offer high range resolution measurements (1 to 30 m) of the lowest kilometre or two of the atmosphere. Their beamwidth resolution typically being around 50 m at 1 km range.

3.2 FACTORS AFFECTING CLEAR AIR RADAR SENSITIVITY

Clear air studies generally involve radar returns from refractive index inhomogeneities. Atlas et al.,(1966b) and more recently Balseley (1978) have discussed the factors affecting the sensitivity of pulsed radars to such returns and Strauch(1976) has detailed the factors affecting FM-CW radar sensitivity. Chadwick and Little (1973) and Ottersten et al.(1973) have compared the sensitivities of a number of clear air radars.

The signal power S received from a target of uniform reflectivity η filling the resolution volume at a range R from a single pulse (or a single sweep in the case of an FM-CW radar) is given by

$$S \sim \frac{P_t \, A_e \, \Delta R}{4 \pi R^2} \eta \tag{2}$$

where P_t is the peak transmitted power (mean power for an FM-CW radar), A_e the effective antenna area and ΔR the range resolution. The noise against which this signal must be detected is given by N = kTB where B is the receiver bandwidth and T the effective noise temperature of the receiver. Depending upon the type of radar employed and on the target characteristics it may be possible to improve the signal to noise ratio by a factor I by a combination of coherent predetection integration, non-coherent integration and spectral processing. If we assume that the minimum detectable signal is obtained when S/N = 1 then

$$\eta_{MIN} \sim \frac{4 \pi R^2 \, k \, T \, B}{P_t \, A_e \, \Delta R \, I} \tag{3}$$

Coherent predetection integration is performed before the radars detector stage and is the most efficient type of integration (Chadwick and Little , 1973). It can be accomplished in an analogue filter or by digital filtering and gives an enhancement proportional to the number of pulses integrated. However.the coherent integration time must be less than both the signal coherence time and the Doppler frequency period of the signal

(Balsley, 1978; Röttger and Schmidt, 1979). These restrictions mean that for a number of radars no predetection integration is possible. Incoherent integration is performed after detection and gives an improvement to the signal to noise ratio proportional to the square root of the number of samples averaged. Doppler processing gives an improvement proportional to the ratio of the unambiguous Doppler velocity range divided by the signal peak spectral width.

In practice idealised signal to noise ratios are not achieved for a variety of reasons. Radars used for clear air studies have very high sensitivities and consequently are susceptible to echoes from ground targets illuminated by the antenna side-lobes. Such ground clutter is most trouble at close ranges. It may be reduced by careful design and suitable siting of the antenna or by electronic filtering. For example the Sunset radar is located in a deep canyon which limits ground returns to 2 km range (Green et al.,1975a). With a coherent radar the Doppler frequency shift may be used to differentiate stationary ground targets from moving clear air ones. Such a technique fails if the signals from the ground returns are sufficiently strong to saturate the rf portion of the receiver. In a pulsed system these circumstances cause the clear air signals to be lost at those ranges for which saturation occurs. In an FM-CW system such circumstances, although harder to realise, cause information to be lost at all ranges (Strauch and Moninger, 1978).

The ability of pulsed radars to operate at short ranges (<1 km) is limited by the requirement to protect the sensitive receiver circuits from the transmitted pulse. In a FM-CW system this restriction does not apply and measurements may be made to ranges as short as a few tens of metres. However the performance of FM-CW radars deteriorates at long ranges as a consequence of unavoidable departures from a perfectly linear sweep of transmitter frequency (Richter et al., 1973a).

Clear air targets generally persist for many tens of seconds so that the amount of integration is not normally limited by the target duration. Non-coherent integration is generally limited by either the requirement to scan the beam or the passage of targets out of the resolution volume. Coherent integration and Doppler processing are limited not only by these requirements but also by the gross motion of the target and its internal motions.

The idealised signal-to-noise equation also assumes that the resolution volume is filled with a distributed target of uniform reflectivity. In practice this assumption is far from the truth as refractive index inhomogeneities are frequently found in thin sheets (typically less than 10 m thick), if such a sheet occupies a fraction of the resolution volume then the signal-to-noise ratio will be reduced by approximately the same fraction.

3.3 METHODS OF PROCESSING ANT DISPLAYING THE RADAR OBSERVATIONS

Recently radars have benefited from the development of systems able to process and display Doppler signals from many range gates in real time. Of the digital spectral analysis techniques Pulse Pair Processing (PPP) and the Fast Fourier Transform (FFT) have found the greatest favour. The PPP technique estimates only the principal Doppler moments whilst the FFT technique provides full spectra at the expense of more elaborate processing (Sirmans and Burmgarner, 1975). The results of PPP analysis can be seriously biased by ground returns and under such circumstances full spectral analysis must be performed. FM-CW Doppler radars also require full spectral processing to obtain Doppler information, there currently being no simple way of extracting the spectral moments (Strauch and Chadwick, 1976).

The output from clear air radars is often displayed on the surface of cathode ray tubes or on photographic strip charts - a degree of incoherent integration being achieved in both cases. More recent systems use digital storage techniques, the results perhaps being manipulated by computer before being output as hard copy or on video displays (refer ahead to Figure 7 for example). Such systems have the advantage that results can be inspected in ambient light and sequences of pictures may be re-played or single frames may be frozen to inspect features of interest.

4. OBSERVATION OF CLEAR AIR PHENOMENA USING NON-DOPPLER RADARS

4.1 DETECTION OF AIR MASS BOUNDARIES

Air mass boundaries have been detected by the presence of both enhanced refractive index inhomogeneities and of insects and birds. Insects can be carried aloft if the boundary between the air masses is a region of convergence and this concentration of food can attract insect eating birds (Eastwood, 1967). In plan view the boundary generally appears as a narrow, often scalloped line echo. Atlas (1960) observed the passage of sea breeze fronts both with a radar and a refractometer and found that the refractive index gradients were sufficiently large to account for the radar returns. Geotis (1964) also observed a number of sea breeze fronts at two wavelengths and concluded that insects and birds were the most probable source of the echoes. It seems likely that in general both types of echo contribute to the returns (Simpson et al., 1977). PPI scans of land breeze fronts (Meyer 1971) have shown scalloped line echoes parallel to the coast and RHI scans indicated that the frontal boundary sloped back towards the land at an angle of about 20°.

Line echoes have been observed at the leading edge of cold outflows associated with thunderstorms (Leach, 1957; Luckenback, 1958; Brown ,1960; Harper 1958, 1960) and dry cold fronts (Ligda and Bigler, 1958). Goff et al. (1977) found that thin radar echo lines ahead of advancing thunderstorms coincided with the leading edge of the outflows but also found that an echo line was not always detectable in association with such outflows. Conversely lines sometimes existed in the absence of nearby storms. Thus the use of thin echo lines as gust front indicators is unreliable in the absence of supporting information.

A warm frontal zone has been observed by a 5.6 m wavelength radar (Röttger ,1979). Operating in a vertically pointing mode the radar clearly observed the advection overhead of a sloping frontal zone. The zone was marked on nearby radiosonde ascents by an inversion. The radar returns may have been due to refractive index inhomogeneities or to partial specular reflection.

4.2 DETECTION OF BOUNDARY LAYER CONVECTION

Clear air echoes are commonly observed in association with convection in cloud free conditions and in precipitation-free cloud. In addition clear air returns can also be distinguished from precipitation by virtue of the different velocities of the hydrometers and the clear air targets (Green et al., 1978a). Early observations showed echoes which in vertical section resembled inverted, U's (Harper et al., 1957; Atlas, 1959) and in horizontal section doughnut rings, Figure 4 (Hardy and Ottersten, 1969; Atlas and Hardy, 1966). The organisation responsible for the production of such domed echoes has been described by Hardy and Ottersten (1969). Warm moist air ascends from the surface in a bubble through cooler and usually drier environmental air and mixing at the interface produces strong refractive index gradients. The strongest echoes are in fact received when the rising bubble has reached a mature stage having overshot the level of neutral buoyancy, the rising air then being cooler as well as moister than the environmental air (Konrad, 1970; Rowland, 1973). The domes are generally 1 to 3 km in diameter and their tops reach similar heights (Atlas and Hardy, 1966; Konrad, 1970). The life cycle of a single convective bubble is about 20 minutes (Hardy and Ottersten, 1969). When observed in horizontal section the ring echoes are frequently found to be organised in rows or streets aligned close to the mean wind direction (Hardy and Ottersten, 1969; Konrad, 1968, 1970). Ring echoes 5 to 10 km in diameter - somewhat larger than those associated with convection - have been attributed to Bénard convection (Hardy and Ottersten, 1969).

The above experiments were performed with high power pulse radars but inverted U echoes have also been observed by fine resolution vertically pointing radars (Gossard et al., 1971). In an experiment involving a FM-CW radar, a high power pulse radar, an acoustic sounder and an instrumented aircraft much was learnt about the processes involved in clear air convection (Richter et al., 1974; Rowland and Arnold, 1975; Arnold et al., 1975; Noonkester and Jensen, 1975; Noonkester, 1976). They discovered that the most active mixing occurred at the top of the convective domes and that the side walls of the inverted Us carry mixing air downwards

(Arnold et al.,1975). Figure 5 shows a temperature sounding obtained with the aircraft through a convective tower observed with the vertically pointing FM-CW radar. It clearly shows the convective turret to consist of cold moist air which has penetrated warm dry environmental air. Such experiments have produced much information clarifying the relationship between the mean rate of rise of the convective tops and the atmospheric stability and heat fluxes (Noonkester, 1976, 1978) a relationship which had previously been examined by Rowland (1973) and Konrad and Robison (1973).

Browning et al. (1973a) combined clear air radar measurements of the convective boundary layer top with measurements from turbulence probes (Readings et al.,1973). They found shearing instability at the crests of convective circulations to be one important mechanism for the transfer of heat and mass across the convective boundary top. On a much broader scale the observations of Harrold and Browning (1971) have shown that the heights reached by convective tops may be considerably modified by topographic effects. Figure 6 shows that on a day with weak winds the depth of the convective boundary layer at midday was clearly related to topography. Two hours later the convection had deepened still further over the high land and eventually thunderstorms developed in these preferred areas. Arnold (1976) has also observed that clear air convection can be triggered in a preferred location, in his case an airfield. Observations showing the depth of the boundary layer over large areas may prove useful in locating regions of low level convergence which precede severe thunderstorms. In typical thunderstorm conditions radars such as the one at Defford (Table 1) can detect the top of the boundary layer out to ranges of 50 to 100 km.

4.3 DETECTION OF ATMOSPHERIC STRATIFICATION

Often the atmosphere becomes organised into a number of thin stably stratified sheets separating thicker layers of lesser stability. These statically stable sheets tend to be regions of strong shear which may lead to local dynamic instability which in turn creates turbulence within the sheets. This turbulence is responsible for the mixing that produces refractive index inhomogeneities on a scale which enables the radar to detect the layers in the first place. If turbulence is generated on scales smaller than the radar resolution volume then plane sheets are observed; if however it is generated on larger scales then modulation of the sheets will be detectable (See Section 4.5). Figure 7 shows a number of layers observed in vertical section at 10 cm wavelength. Some studies have involved simply locating these stable layers, some have concentrated on the structure of such layers (Metcalf and Atlas, 1973), whilst others have used the perturbation of the height of such layers as indicators of wave motion (eg Bean et al., 1973) or the upward penetration of convection (eg Browning et al., 1973a).

One feature of atmospheric stratification of considerable interest is the tropopause. This was first observed as a layer echo using 10 and 71 cm wavelength radars. (Atlas et al., 1966a). The wavelength dependence of the layer reflectivity was consistent with reflection from refractive index inhomogeneities. Gage and Green (1979) have examined the radar returns obtained from heights near the tropopause at vertical and oblique incidence at 7.4 m wavelength. After range normalizing their results they found enhanced reflectivity from certain layers at vertical incidence which they attributed to specular reflection from stable layers in the lower stratosphere. Stable layers appear to be common both in the high troposphere and low stratosphere and it is not always clear which of these layer echoes is associated with the tropopause.

The most detailed observations of stable layers have been made with vertically pointing FM-CW radars. Richter (1969), using a 1 m resolution sounder, examined echoes associated with temperature inversions and found that often several echo layers were present within an inversion. Generally the strongest and most persistent echo was found at the inversion base in association with maxima in the mean vertical gradient of refractivity as measured by an in-situ probe. Other echo layers, generally weaker and less persistent, were found higher in the inversions associated with sharp changes in the vertical gradient of refractivity.

Both low level fog and stratus tend to be capped by sheared stable layers which may be detected by radar. Thin echo layers have been observed at the top of advection fog (Noonkester et al., 1974, 1976a,b) and stratus clouds below 600 m (Richter et al.,1973a; Noonkester et al., 1974, 1976a). The clouds disperse when the cloud top temperature inversion weakens and the thin echo layers become more diffuse before disappearing.

4.4 DETECTION OF GRAVITY WAVES

In the early 1970s Gossard, Jensen and Richter documented numerous examples of thin echo layers distorted by gravity waves and were able to account theoretically for many of the striking features they observed (Gossard and Richter ,1970, 1972; Gossard et al.,1970,1971, 1973). The observations stimulating their work were principally fine-resolution vertically-pointing FM-CW radar measurements made within the first kilometre of the atmosphere. Figures 8 and 9 show examples of two types of gravity wave studied. In Figure 8 the periodically spaced sloping layers are considered to be caused by untrapped internal gravity waves whose propagation vector is nearly vertical (Gossard et al., 1971). Figure 10 shows an example of a trapped internal gravity wave (Gossard and Richter, 1970), the pointed crests and flattened throughs being due to non linear effects caused by the proximity of the ground.

One disadvantage of vertically pointing observations of gravity waves is that additional information, perhaps from a microbarograph array, is required before certain wave parameters such as wavelength and direction of propagation may be estimated. This disadvantage may be overcome with a scanning radar. Figure 10 is a sequence of RHI scans showing a number of clear air layers modulated by mountain lee waves (Browning, 1978). This particular train of waves was stationary and relatively undamped with distance downstream. On other occasions Starr and Browning (1972) observed damped or transient lee waves.

4.5 DETECTION OF SHEARING INSTABILITIES

The observation of clear air echo layers is possible as a result of turbulence suspected to have been generated by shearing instability on scales smaller than the radar resolution. If the instability occurs also on larger scales then its structure may be directly observed with radars.

As mentioned before, Hicks and Angell (1968) observed echo patterns which in vertical section resembled a braided rope. An example of such a braided echo is shown in Figure 11 (Browning, 1971). This particular disturbance had a crest-to-trough amplitude of 400 m and a wavelength of 1.5 km. Such a pattern is just one stage in the evolution of Kelvin-Helmholtz (K-H) shearing instability. The train of events accompanying such breaking K-H billows has been observed by Browning and Watkins (1970) and Gossard et al. (1971). Figure 12 clearly shows, from left to right, the development of a 100 m amplitude billow, its breaking and its subsequent decay (Gossard et al., 1971). Theory (Miles and Howard, 1964) and observation (Browning, 1971) both suggest that K-H instability develops when the Richardson number over a layer falls below a critical value of 1/4.

Figure 13 shows billows of a few metres amplitude outlining a gravity wave of 25 m amplitude. The billows are themselves made visible to the 10 cm wavelength radar by virtue of motions on yet smaller scales which produce refractive index inhomogeneities on a scale of half the radar wavelength.

Joint studies involving aircraft together with clear air radars have shown that large amplitude billows are a cause of clear air turbulence (CAT). Browning et al. (1970), for example, measured moderate turbulence associated with 500 m amplitude billows. Aircraft equipped to measure air velocities and temperature have also been flown through billows being detected by radar enabling detailed models of the instability to be developed (Hardy et al., 1973; Browning et al., 1973b). Browning et al. (1973b) in fact slaved the radar to closely follow the aircraft motion to ensure that both made measurements in the same region of the atmosphere.

5. THE MEASUREMENT OF THE KINEMATIC STRUCTURE OF THE CLEAR ATMOSPHERE MAINLY USING DOPPLER TECHNIQUES

5.1 MEASUREMENTS OF WINDS AND WIND FIELDS

Wind fields have been obtained at all heights in the troposphere by observing clear air targets. Wind measurements using a single Doppler radar have generally been made using observations at one or two azimuths (Green et al., 1975b, 1978a; VanZandt et al., 1975) or by conical scans (scanning in azimuth at a fixed elevation angle) (Lhermitte and Atlas, 1961; Browning and Wexler, 1968). Some results obtained using the former technique are shown in figure 14 which shows radial velocity spectra taken with the Sunset radar at an elevation angle of 60°. (VanZandt et al., 1978). The range resolution was 1 km and each spectrum was accumulated over a period of 50 seconds. The numbers on the left give the integrated signal-to-noise ratio, defined as the ratio of the signal power under a peak to the total noise power across the whole spectrum. It can be seen that velocity measurements are still possible, in this case up to 14 km, even when this ratio has fallen below unity by virtue of Doppler processing. The data were taken during the passage of a polar front jet stream and if it is assumed that vertical velocities are negligible, the data indicate a maximum velocity component of 65 ms^{-1} at around 10 km. Similar results have been obtained with the Poker Flat radar (Ecklund et al., 1977). Both the Sunset and Poker Flat radars have antennae constructed from dipole arrays and are able to make observations in only a limited number of preset directions. Continuously steerable dishes such as that at Chatanika and the fixed dish/steerable feed system at Arecibo permit more flexible scanning procedures. Both these radars have been used to observe tropospheric winds using conical scans. (Balsley et al., 1977; Farley et al., 1979). Such scans give more representative measurements of the vertical profile of the horizontal wind than observations in a few directions. Figure 15 shows two wind profiles obtained using conical scans with the Chatanika radar (Balsley et al., 1977). Each scan took around 12 minutes and results were obtained with a 1 km vertical resolution. The wind obtained from a nearby radiosónde ascent demonstrates the good accuracy obtained. Vertical air velocities have also been estimated by integrating the divergence measured in a number of conical scans at different altitudes (Balsley et al., 1977) as well as by direct observations at vertical incidence (Green et al., 1978a; Röttger et al., 1978). Such experiments to measure vertical air velocities must be carefully designed so that short period gravity waves do not bias the results.

Currently the more sensitive radars are able to obtain wind soundings throughout the entire depth of the troposphere at resolutions of a few hundred metres in a period of a minute or so. However within the boundary layer reflectivities are large enough to enable velocity measurements to be made at resolutions of a few tens of metres in a few seconds. Figure 16 shows some measurements of wind velocity taken over consecutive ten second intervals of time at 32 m resolution in the boundary layer (Chadwick et al., 1976).

The availability of continuous wind soundings permits studies of pehnomena such as low level jets, gust fronts, waves and boundary layer circulations. Figure 17 shows the velocity structure of a low level jet over a period of 24 hours determined using conical scans (Lhermitte, 1966). The targets in this case are thought to have been primarily insects and their presence enabled measurements to be made with a radar of modest sensitivity. More recently developed radars need not rely on the fortuitous presence of such targets. An example of results obtained in clear air conditions is shown in Figure 18 (Lee and Goff, 1976). It shows radial velocities measured during an RHI scan normal to a thunderstorm gust front. The negative velocities near the ground are towards, and the positive ones above away from the radar. Similar scans at a number of different azimuths enabled a 3 dimensional picture of the shape of the gust front boundary to be produced. Velocity measurements in the vicinity of large amplitude Kelvin-Helmholtz waves have been reported by Browning et al.(1973b). Although the data were of relatively course resolution they were able to reveal regions of concentrated vertical wind shear associated with individual billows. Gravity waves have been detected with Doppler radars by Röttger et al.(1978) and VanZandt et al.(1979). Both used measurements obtained in a single direction and observed the modulation the waves applied to the line of sight velocity at a number of ranges.

Individual radars using relatively simple scans produce valuable results, particularly in the middle and upper troposphere; however, in the boundary layer wind fields show considerably more small scale spatial variability and there is a requirement to obtain 2 and 3 dimensional velocity fields. In an early experiment Frish and Chadwick (1975) used two Doppler radars sited 16 km apart to observe chaff as a tracer of airflow within the otherwise clear convective boundary layer. Although the measurements were limited to a volume 5 km by 5 km in area and 1 km deep, they nevertheless were interesting in that they showed vortex structures within the boundary layer. These had horizontal dimensions of about 2 km, vertical dimensions of 1 km and vertical velocities, derived using the equation of continuity, of about 1 ms^{-1} (Frish et al.,1976). Similar studies also utilising chaff as a tracer have been performed by Kropfli and Kohn (1976) and Gossard and Frish (1976).

A clear air dual Doppler system has been developed using two weather radars of modest power 40 km apart in Oklahoma (O'Bannon,1978; Doviak and Jobson,1979). (see entry for Norman radar in table 1). Each radar is sufficiently sensitive to obtain clear air velocities to heights of 1 to 2 km at ranges as large as 50 km. A coordinated scan with the two radars overs an area 25 by 25 km. A scan covering this region with horizontal and vertical resolutions of 500 m and 250 m, respectively, takes 5 minutes. Figure 19 is a vertical section presenting a sample of the kind of results that can be obtained (Berger and Doviak, 1979). It shows organized circulations within the boundary layer. Such an observational technique has considerable potential to aid our understanding of the dynamics of the boundary layer.

5.2 MEASUREMENTS OF TURBULENCE AND FINE SCALE WIND STRUCTURE

Radar measurements in the clear air have been used in a variety of ways to observe wind fluctuations and to estimate the intensity of turbulence. The most direct method of observing larger scale fluctuations is to detect changes in the measured velocities from one time and from one resolution volume to the next. Turbulence on scales smaller than the resolution volume has been estimated from the width of the Doppler spectral peak and also from the intensity of the clear air returns themselves.

a) TURBULENCE ESTIMATES USING THE DOPPLER PEAK WIDTHS

Turbulence on scales smaller than the resolution volume causes a broadening of the Doppler velocity spectra. The contribution of turbulence to the spectral variance, σ^2_{turb}, has been related by Frish and Clifford (1974) to the rate of dissipation of turbulent kinetic energy, ϵ, assuming that the inertial subrange extends to scales the size of the resolution volume. They find that ϵ is proportional to $(\sigma^2_{turb})^{3/2}$. The observed spectral variance σ^2_{obs} is given by

$$\sigma^2_{obs} = \sigma^2_{shear} + \sigma^2_{turb} + \sigma^2_{beam} + \sigma^2_{inst} + \sigma^2_{temp} \qquad (4)$$

where σ^2_{shear} is the contribution due to both radial and transverse shear, σ^2_{beam} is the beam width broadening term, σ^2_{inst} is the contribution of instrumental and signal processing broadening and σ^2_{temp} allows for the temporal variation of mean wind speed within the pulse volume.

Thus in order to obtain σ^2_{turb} these other contributions must be either measured or estimated. The requirement that the inertial subrange extends to scales the size of the resolution volume means that this technique can only reliably be used with high resolution radars.

The technique has been used by Moninger et al. (1978) and Hildebrand (1976) to measure turbulence within clouds of chaff dispersing in the boundary layer. Figure 20 shows estimates of ϵ obtained from clear air measurements of σ^2_{obs} across an inversion (Gossard et al., 1978). The results show that ϵ peaks a little way below the inversion base.

b) TURBULENCE ESTIMATES USING C_n^2

In stable conditions the relationship between C_n^2 and turbulence involves the vertical gradient of refractive index and the vertical wind shear (Ottersten, 1968, 1969a,b)

$$C_n^2 = a^2 \epsilon^{\frac{2}{3}} \left(\frac{dn}{dz}\right)^2 \left(\frac{du}{dz}\right)^{-2} \qquad (5)$$

Despite this additional dependance, Ottersten (1969a) and more recently Gage and Balsley (1978) and Green et al. (1978b) consider that C_n^2 itself (inferred from η using equation (1) may be used as an indicator of the intensity of turbulence. However, as Gage and Balsley point out, such a method is only likely to give an accuracy of around an order of magnitude. In Figure 20 it can be seen that C_n^2 derived from η and ϵ derived from σ^2_{obs} reach maximum values at different heights. The peak value of C_n^2 is in fact obtained at the height at which the vertical gradient of refractive index, $\frac{dn}{dz}$, is a maximum. In this case $\frac{dn}{dz}$ is dominated by the vertical gradient of water vapour pressure.

Ottersten (1968) argues that this technique is most appropriate for the detection of clear air turbulence at high altitudes where temperature gradients dominate the refractive index gradient. In a combined aircraft/radar experiment Glover and Duquette (1970) found that all the layer echoes observed with the Wallops Island radars, when probed by an aircraft proved to be turbulent. However, only below 3 km height were all cases of aircraft turbulence found to correspond to clear air layers. At higher altitudes it was suggested that the refractive index gradients tended to be smaller and so a given amount of turbulence gave a smaller radar reflectivity. The use of Cn^2 as a measure of turbulence also requires that signals from other targets, such as cirrus clouds, be discriminated against. Whilst this can be done, by using measurements at two wavelengths for example, this is not a cost effective approach especially bearing in mind that the results will be obtained only over a limited geographical area (Watkins and Browning 1973).

c) ESTIMATES OF WIND FLUCTUATIONS USING MEAN DOPPLER VELOCITY MEASUREMENTS

At present the most reliable method of detecting turbulent wind fluctuations is by examining features in the field of mean velocity. Such a method gives direct information on the air motion only on scales larger than the radar resolution volume. Figure 16 shown earlier gives four consecutive wind profiles obtained in the boundary layer (Chadwick et. al.,1976). The wind can be seen to change rapidly in the height interval between 150 and 300 m. A sequence of this type of observation obtained at one second intervals is shown in Figure 21. (James et al.,1978). The line-of-sight velocity measurements were obtained using the Defford radar at an elevation angle of 3°. Superimposed on the velocity field is the path of a hypothetical aircraft taking off at 70 ms^{-1}. Between points b and c the wind speed increases by 5 ms^{-1} in a flight time of $\frac{1}{2}$ second. Such observations with Doppler radars are one of a number of techniques being developed for the observation of hazardous wind shears which can affect aircraft landing or taking off (Strauch and Moninger, 1978). Berger and Doviak (1979) have studied quantitatively the turbulent structure of the boundary layer using the dual Doppler radar system in Oklahoma. On an occasion when they observed well developed roll structures with horizontal and vertical dimensions of 5 and 2.5 km respectively, they found that the -5/3 spectral law applied on scales up to about 2 km.

6. PROMISING APPLICATIONS

The observation of the troposphere under clear air conditions using sensitive radars has so far been almost entirely a research activity. However there is now interest in exploiting such radars for operational uses. The two areas most likely to benefit from such efforts are the measurement of vertical wind profiles and the detection of hazardous low level wind shears.

Passive microwave sounders are able to obtain vertical temperature and humidity profiles and large pulsed radars can provide continuous vector wind measurements throughout the troposphere under all weather conditions. Thus it has been proposed that it might eventually become economic to replace radiosonde ascents by remote sounders able to produce continuous profiles unattended. As well as enhancing the synoptic network and improving the possibilities for local forecasting, such observations would also permit further detailed studies to be made of mesoscale phenomena.

For the detection of hazardous low level wind shear, radar has the advantage over current optical and acoustic sounders of all weather performance. Pulsed Doppler radars appear to be more suitable for such observations than FM-CW ones as the latter have yet to demonstrate their ability to operate at very low elevation angles and at large ranges. However, pulsed radars are not without their problems. Careful siting is required both to minimise ground returns and to satisfy airport safety regulations. In addition current pulsed systems have minimum ranges as great as 1 km, determined by receiver recovery time. But the main difficulties to overcome are likely to be the development of a suitable strategy for collecting observations which can provide a timely warning of hazardous shears and the dissemination of such information to pilots and controllers.

Another area in which clear air observations might be used operationally in the longer term is to help in the early identification of the preferred regions for outbreaks of severe local storms. Low level convergence which precedes the development of such storms has been detected using a single radar by the direct observation of the increase in the height of the convective boundary layer. In the future the magnitude of such convergence could be measured using dual Doppler radars. Such a scheme would require rapid processing of large quantities of data and the optimisation of criteria designed to pinpoint preferred areas of storm development.

ACKNOWLEDGEMENTS

The author would like to express his gratitude to K.A.Browning for his helpful advice and constructive criticism offered throughout the preparation of this paper.

FIGURE CAPTIONS

Figure 1 Vertical profile of C_n^2 averaged over a period of 36 minutes obtained with the Poker Flat phased array radar in Alaska. The average value of C_n^2 decreases by more than two orders of magnitude between 2 and 8 km height. (After Ecklund et al.,1977).

Figure 2 Statistics of C_n^2 obtained over a period of one year in Colorado. The figure shows as a function of time of day the percentage of observations which were less than given values of C_n^2. The data were collected at a height of 805 m with time and height range resolution of 1 minute and 160 m respectively. (Chadwick et al., 1978b).

Figure 3 Time-height observations of reflectivity made at vertical (VE) and oblique (OB, 12.5^o off the zenith) incidence with the 5.6 m wavelength SOUSY radar. The reflectivity of particular layers at around 3 km height was 20 dB higher in the vertically pointing mode (Röttger and Liu,1978).

Figure 4 Photograph of the PPI display of the 10 cm radar at Wallops Island, obtained with the beam at an elevation of 3^o, showing characteristic doughnut-shaped echoes where the beam intersects the upper parts of inverted U-shaped convective cells (Hardy and Ottersten,1969).

Figure 5 Observations of a convective turret made with vertically pointing FM-CW radar (top) and instrumented aircraft (middle and bottom). The aircraft track is marked on the FM-CW photograph and the temperature and humidity records show the turret to consist of air cold and moist relative to the environment. (Arnold et al.,1975).

Figure 6 The depth of the convective boundary layer as determined by the high-power radar at RSRE Defford at about midday on 10 June 1970 is shown ~~on~~ the right. The area of deeper convection coincides with the high land of the Costwolds shown on the left. Two hours later the boundary layer had deepened to 3 km over the Cotswolds and after a further two hours thunderstorms broke out (after Harrold and Browning, 1971).

Figure 7 Black and white photograph of the intensity modulated RHI display of the 10 cm radar at RSRE Defford at 15.20 GMT on 17 July 1979. The display shows horizontal stable layers at heights of 1.6, 1.9 and 2.2 kms. Information for the display is processed digitally and presented on a colour television monitor.

Figure 8 Periodically spaced sloping layers observed with a vertically pointing FM-CW radar. The layers are thought to be caused by untrapped internal gravity waves whose propagation vector is nearly vertical.(Gossard et al.,1971).

Figure 9 An internal gravity wave observed with a vertically pointing FM-CW radar. The pointed crests and flattened troughs arise as a result of non linear effects due to the proximity of the ground (Gossard and Richter,1970).

Figure 10 Sequence of three photographs of the RHI display of the RSRE Defford radar, obtained on 22 April 1970, showing stationary lee waves downwind of the hills of South Wales. The RHI sections were obtained at 6 minute intervals looking into the wind along 250°. Below 3 km the echoes are from the clear air and they show a standing-wave pattern with waves decreasing from a maximum crest-trough amplitude of 600 m over the hills at 70 km range to less than 200 m near the radar. Above 3 km the echoes are from streamers of ice crystals and recognisable features can be

Figure 10 (Continued)	seen travelling towards the radar at almost 30 ms^{-1}. Between 0908 and 0914 GMT the streamer identified by an asterisk can be seen ascending from a trough to a crest in the lee wave pattern (Browning, 1978).
Figure 11	Photograph of the RHI display of the RSRE Defford radar, showing Kelvin-Helmholtz billows appearing like a braided rope at an altitude of 5 to 6 km. Echoes from the top of the convective boundary layer and from an inversion can be seen at 1 and 2 km, respectively. Range rings are present at 5 and 10 km. (from Browning, 1971).
Figure 12	A time-height observation of Kelvin-Helmholtz shearing instability made with a vertically pointing 10 cm FM-CW radar. The sequence, from left to right, shows the growth of a billow, its breaking and subsequent decay (Gossard et al., 1971)
Figure 13	Two time-height photographs of the same data obtained with a vertically pointing FM-CW radar. The upper picture clearly shows trains of gravity waves with amplitudes of around 25 m. At reduced exposure Kelvin-Helmholtz billows of a few metres amplitude are seen to outline the uppermost gravity wave. The sloping lines are returns from a nearby captive balloon. (Gossard et al., 1973).
Figure 14	Radial velocity spectra as a function of height, indicated on the right, measured by the Sunset radar on 15 April 1976, 2306Z. The phased array antenna was tilted 30° off zenith. The data indicate a velocity maximum of 65 ms^{-1} at 10 km height. The figures on the left give the integrated signal-to-noise ratio for each spectrum, defined as the ratio of the signal power under a peak to the total

Figure 14 (Continued) noise power across the whole spectrum. (VanZandt et al.,1978)

Figure 15 Two vertical profiles of wind speed and direction obtained with the Chatanika radar using conical scans. Each scan took around 12 minutes. Also shown is the wind profile measured from a conventional radiosonde ascent. (Balsley et al., 1977).

Figure 16 Four consecutive wind profiles along 315° obtained with a Doppler FM-CW radar at an elevation angle of 60° (Chadwick et al.,1976).

Figure 17 Velocity structure of a low level jet obtained over a period of 24 hours using conical scans. The targets in this case are likely to have been primarily insects (after Lhermitte, 1966).

Figure 18 Clear air velocities measured during an RHI scan normal to a thunderstorm gust front. Velocities towards the radar are shaded (Lee and Goff, 1976).

Figure 19 A vertical section displaying air velocities deduced from dual Doppler clear air measurements. The radars at Norman and Cimarron are scanned to obtain the horizontal line of sight velocity in a number of vertically stacked horizontal planes. The equation of continuity can then be used to calculate vertical velocities as displayed above (Berger and Doviak, 1979).

Figure 20 Vertical profiles of C_n^2 (derived from η) and ϵ (derived from σ^2) obtained with a vertically pointing FM-CW radar. Also shown are temperatures and winds measured by a nearby radiosonde ascent. (Gossard et al.,1978).

Figure 21 Clear air Doppler velocity measurements obtained with the RSRE Defford radar operating at an elevation angle of 3° into the wind. Velocities were extracted at intervals of 1 second in time and 30 m in range. The white arrow superimposed on the velocity field is the path of a hypothetical aircraft taking off at 70 ms^{-1}. Between points b and c the wind speed increases by 5 ms^{-1} in a flig time of $\frac{1}{2}$ second (James et al., 1978).

TABLE CAPTION

Table 1. The characteristics of a number of radars used for clear air research in the last decade. Some of the characteristics, for example range resolution and integration times, may be changed for different experiments.

There is no satisfactory way of comparing the sensitivities of clear air radars operating on different wavelengths with resolution volumes of widely differing sizes. However the minimum C_n^2 values above have been calculated for typical experimental conditions. Problems involved in comparison include:

i) Radars use different integration times. For example the minimum C_n^2 values for the Norman, Defford and SOUSY radars assume an observational period of 100 msec and a target whose Doppler velocity speed is 2 ms^{-1}, in contrast the figures for Chatanika, Poker Flat and Sunset assume the same Doppler velocity speed but an observational period of 60 seconds.

ii) The use of a minimum detectable C_n^2 implies a resolution volume filling turbulent target. Such a condition is unlikely to be realised in practice as turbulence is generally confined to thin sheets. This particular condition endows the coarse range resolution radars with greater apparent sensitivity.

(iii) At wavelengths greater than about 1 m cosmic noise generally exceeds receiver noise and this noise varies with time of day and radar attitude.

(iv) A minimum detectable C_n^2 is not an appropriate parameter to use when comparing radars used to observe partial specular reflection.

In order to overcome some of these problems Gage and Balsley (1978) have suggested that the Average Power Aperture Product ($\overline{P}_t . A_e$) be used to compare the sensitivity of different radars to turbulent scattering and Röttger (personal communication, 1979) suggests that $\overline{P}_t . A_e^2$ be used to compare the sensitivity of radars to partial specular reflection.

REFERENCES

Arnold A. 1976 'Observation of the Development of Individual Clear Air Convective Cells', Reprints 17th Radar Meteorol.Conf., Amer.Meteorol.Soc.,Boston,338-341.

Arnold A., J.R. Rowland,T.G.Konrad., J.H.Richter, D.R. Jensen, and V.P.Noonkester. 1975 'Simultaneous Observations of Clear Air Convection by a pulsed Radar, an FM-CW radar, an Acoustic Sounder and an instrumented aircraft', Reprints 16th Radar Meteorol.Conf., Amer. Meteorol.Soc.,Boston, 290-295.

Atlas D. 1959 'Meteorological Angel Echoes', J.Meteorol., 16, 6-11.

Atlas D. 1960 'Radar Detection of the Sea Breeze', J. Meteorol., 17, 244-258.

Atlas D. 1964 'Advances in radar meteorology', Advan. Geophys., 10, 317-478.

Atlas D., and K.R. Hardy 1966 'Radar analysis of the clear atmosphere: Angels', Proc.XV General Assembly of URSI,Munich 5-15 Sept., 401-469.

Atlas D., K.R. Hardy, and T.G. Konrad 1966a 'Radar detection of the tropopause and clear air turbulence', Proc. 12th Weather Radar Conf., Amer. Meteorol.Soc., Boston, 279-284.

Atlas D., K.R.Hardy, and K.Naito 1966b 'Optimizing the Radar Detection of Clear Air Turbulence', J.Appl.Meteorol., 5, 450-460.

Balsley B.B. 1978 'Design considerations for coherent radar systems for probing the troposphere. stratosphere, and mesosphere', Reprints 18th Conf.Radar Meteorol., Amer.Meteorol.Soc., Boston, 387-390.

Balsley B.B., N. Cianos, D.T.Farley, and M.J.Baron 1977 'Winds derived from radar measurements in the Arctic troposphere and stratosphere', J.Appl.Meteorol., 16, 1235-1239.

Battan L.J. 1973 'Radar observations of the Atmosphere', 324 pp., The University of Chicago Press.

Bean B.R. and E.J.Dutton 1968 'Radio Meteorology', 435pp, Dover, New York.

Bean B.R., R.E.McGavin, R.B.Chadwick, and B.D.Warner 1971 'Preliminary Results of Utilizing the high resolution FM Radar as a boundary layer Probe', Boundary-layer Meteorol., 1,466-473.

Bean B.R., R.E.McGavin, and B.D. Warner — 1973 — 'A Note on the FM-CW Radar as a Remote Probe of The Pacific Trade-Wind Inversion', Boundary-layer Meteorol., 4, 201-209.

Berger M.I. and R.J. Doviak — 1979 — 'An Analysis of the Clear Air Planetary Boundary Layer Wind Synthesized from NSSL's Dual Doppler Radar Data', NOAA Tech.Memo. ERL-NSSL-86, National Severe Storms Laboratory, NOAA, Norman, Oklahoma, 73069.

Brown H.A. — 1960 — 'Report on radar thin lines', Proc. 8th weather Radar Conf., Amer. Meteorol.Soc., Boston, 65-72.

Browning K.A. — 1971 — 'Structure of the Atmosphere in the Vicinity of large-Amplitude Kelvin-Helmholtz Billows', Quart.J.Roy.Met.Soc., 97, 283-299.

Browning K.A. — 1978 — 'Meteorological aspects of radar', Rep.Prog.Phys., 41, 761-806.

Browning K.A. and D.Atlas — 1966 — 'Velocity characteristics of some clear air dot angels', J.Atmos.Sci., 23,592-604.

Browning K.A. and C.D.Watkins — 1970 — 'Observations of Clear Air Turbulence by High Power Radar', Nature, 227, 260-263.

Browning K.A. and R.Wexler — 1968 — 'A determination of kinematic properties of a wind field using Doppler radar' J.Appl. Meteorol., 7,105-113.

Browning K.A., C.D.Watkins, J.R.Starr and A. McPherson — 1970 — 'Simultaneous Measurements of Clear Air Turbulence at the Tropopause by High-Power Radar and Instrumented Aircraft', Nature, 228,1065-1067.

Browning K.A., J.R. Starr and A.J.Whyman — 1972 — 'Measurements of air motions in regions of clear air turbulence using high power Doppler radar', Nature, 239, 267-269.

Browning K.A., J.R. Starr and A.J.Whyman — 1973a — 'The structure of an Inversion Above a Convective Boundary Layer as Observed Using High Power Pulsed Doppler Radar', Boundary-Layer Meteorol., 4, 91-111.

Browning K.A., G.W.Bryant, J.R.Starr, and D.N.Axford — 1973b — 'Air Motion within Kelvin-Helmholtz billows determined from simultaneous Doppler radar and aircraft measurements'. Quart. J.Roy.Met. Soc.,99, 608-618.

Chadwick R.B. and C.G.Little 1973 'The comparison of sensitivities of atmospheric echo-sounders', Remote Sensing of the Environment, 2, 223-234.

Chadwick R.B., K.P. Moran, R.G.Straugh, G.E.Morrison and W.C.Campbell 1976 'Microwave radar wind measurements in the clear air', Radio Sci., 11, 795-802.

Chadwick R.B., K.P.Moran and G.E.Morrison 1978a 'Measurements towards a C_n^2 Climatology', Reprints 18th Conf. Radar Meteorol., Amer.Meteorol.Soc., Boston, 100-103.

Chadwick R.E., K.P.Moran, G.E.Morrison and W.C.Campbell 1978b 'Measurements showing the feasibility for radar detection of hazardous wind shear at airports', Report No. AFGL-TR-78-0160, Wave Propagation Laboratory, Boulder, Colorado 80302.

Dobson E.B. 1970 'Doppler radar measurements of mean wind variations in the clear atmosphere', Reprints 14th Radar Meteorol. Conf. Amer.Soc., Boston, 69-78.

Doviak R.J. and C.T.Jobson 1979 'Dual Doppler Radar Observations of Clear Air Wind Perturbations in the Planetary Boundary Layer', J.Geophys. Res., 84, 697-702.

Eastwood E. 1967 'Radar Ornithology', 278pp., Methuen, London.

Ecklund W.L., D.A.Carter and K.S. Gage 1977 'Sounding of the lower atmosphere with a portable 50 MHz coherent radar', J.Geophys.Res., 82, 4969-4971.

Farley T.F., B.B. Balsley, W.E. Swartz and C.Lahoz 1979 'Tropical Winds measured by the Arccibo Radar', J.Appl.Meteorol., 18, 227-230.

Frish A.S., and S.F.Clifford 1974 'A study of Convection Capped by a Stable Layer Using Doppler Radar and Acoustic Echo Sounders', J.Atmos.Sci., 31, 1622-1628.

Frish A.S. and R.B.Chadwick 1975 'Observations of velocity fields and velocity spectra in the convective boundary layer using a dual-doppler radar system', Preprints 16th Radar Meteorol.Conf., Amer.Meteorol Soc., Boston, 237-242.

Frish A.S., R.B. Chadwick, W.R. Moninger and J.M.Young 1976 'Observations of Boundary Layer Convection Cells Measured by Dual-Doppler Radar and Echosonde and by Microbarograph Array', Boundary-Layer Meteorol., 10, 55-68.

Gage K.S. and B. B. Balsley 1978 'Doppler Radar probing of the clear Atmosphere', Bull. Amer. Meteorol.Soc., 59, 1074-1093.

Gage K.S. and J.L. Green	1979	'Tropopause Detection by Partial Specular Reflection using VHF Radar', Science, 203, 1238-1240.
Geotis S.G.	1964	'On Sea Breeze Angels' Proc. 11th Weather Radar Conf., Amer. Meteorol.Soc., Boston, 6-9.
Glover K.M. and E.F. Duquette	1970	'A study of Clear Air Turbulence using Sensitive Radars', Preprints 14th Radar Meteorol. Conf., Amer.Meteorol.Soc.,Boston, 89-94.
Glover K.M. and K.R.Hardy	1966	'Dot Angels: Insects and Birds', Proc. 12th Weather Radar Conf., Amer.Meteorol.Soc.,Boston, 264-268.
Goff R.C., J.T. Lee and E.A. Brandes	1977	'Gust Front Analytical Study Report No. FAA-RD-77-119, Federal Aviation Administration, Systems Research and Development Service, Washington, D.C. 20590.
Gossard E.E.	1977	'Refractive Index Variance and its height distribution in different air masses', Radio Sci., 12, 89-105.
Gossard E.E.	1978a	'The distribution of radio refractive index structure parameter in boundary layers undergoing spatial or temporal transition', Radio Sci., 13, 255-259.
Gossard E.E.	1978b	'The height distribution of refractive index structure parameter in an atmosphere being modified by spatial transition at its lower boundary', Radio Sci., 13, 489-500.
Gossard E.E. and A.S.Frisch	1976	'Kinematic models of a dry convective boundary layer compared with Dual Doppler radar observations of wind fields', Boundary-Layer Meteorol., 10, 311-330.
Gossard E.E. and J.H. Richter	1970	'The shape of Internal Waves of Finite Amplitude from High Resolution Radar Sounding of the Lower Atmosphere', J.Atmos.Sci., 27, 971-973.
Gossard E.E. and J.H.Richter	1972	'FM-CW Radar Studies of Production of Turbulent Instability within Thermally Stable Layers by Internal Waves', in Effects of Atmos.Gravity Waves on Electromag. Wave Prop., AGARD Conf. Proc., 115, Wiesbaden, Germany. Ref.No.20,14pp.

Gossard E.E., J.H.Richter and D. Atlas | 1970 | 'Internal waves in the Atmosphere from High-Resolution Radar Measurements', J.Geophys. Res., 75, 3523-3536.

Gossard E.E., D.R.Jensen and J.H.Richter | 1971 | 'Analytical study of Tropospheric structure as seen by high-resolution radar', J.Atmos. Sci., 28, 794-807.

Gossard E.E., J.H.Richter and D.R. Jensen | 1973 | 'Effect of wind shear on atmospheric wave instabilities revealed by FM-CW radar observations', Boundary-layer Meteorol., 4, 113-131.

Gossard E.E., R.B.Chadwick, K.P.Moran, R.G. Strauch, G.E.Morrison and W.C.Campbell | 1978 | 'Observations of winds in the clear air using FM-CW radar', Radio Sci., 13, 285-289.

Green J.L., J.M.Warnock, R.H.Winkler, and T.E.VanZandt | 1975a | 'A sensitive VHF radar for the study of winds, waves and turbulence in the troposphere, stratosphere and mesosphere' Reprints 16th Radar Meteorol.Conf., Amer. Meteorol.Soc., Boston, 313-315.

Green J.L., J.M.Warnock, R.H.Winkler and T.E.VanZandt | 1975b | 'Studies of winds in the upper troposphere with a sensitive VHF radar', Geophys.Res.Lett., 2, 19-21.

Green J.L., R.H. Winkler, J.M. Warnock, W.L. Clark, K.S. Gage and T.E.VanZandt | 1978a | 'Observations of enhanced clear air reflectivity associated with convective clouds', Preprints 18th Conf. Radar Meteorol., Amer.Meteorol.Soc., Boston, 88-93.

Green J.L., K.S. Gage and T.E.VanZandt | 1978b | 'VHF Doppler Radar Studies of CAT in the Troposphere and Lower Stratosphere', Preprints Conf. on Atmos. Environment of Aerospace Systems and Applied Meteorology N.York., 159-164.

Hardy K.R. | 1972 | 'Studies of the clear atmosphere using high power radar', Remote Sensing of the Troposphere, ed. by V.E.Derr, chap. 14, NOAA, Washington D

Hardy K.R. and I. Katz | 1969 | 'Probing the Clear Atmosphere with High Power High Resolution Radars', Proc. IEEE, 57, 468-480.

Hardy K.R. and H.Ottersten | 1969 | 'Radar Investigations of Convective Patterns in the Clear Atmosphere, J.Atmos. Sci., 26, 666-672.

Hardy K.R., D. Atlas and K.M. Glover | 1966 | 'Multiwavelength backscatter from the clear atmosphere', J.Geophys. Res., 71, 1537-1552.

Hardy K.R., J.R. Reed and G.K Mather | 1973 | 'Observations of Kelvin-Helmholtz billows and their mesoscale environment by radar, instrumented aircraft, and a dense radiosonde network', Quart. J.Roy.Met. Soc., 99, 279-293.

Harper W.G. | 1958 | 'Detection of bird migration by centimetric radar: A cause of radar angels', Proc. Roy.Soc., B149, 484-502.

Harper W.G. | 1960 | 'An unusual indicator of convection' Marine Observer, 30, 36-40.

Harper W.G., F.H. Ludlam and P.M.Saunders | 1957 | 'Radar Echoes from Cumulus Clouds' Proc. 6th Weather Radar Conf., Amer.Meteorol.Soc., Boston,267-273.

Harrold T.W. and K.A.Browning | 1971 | 'Identification of preferred areas of shower development by means of high power radar', Quart. J.Roy.Met. Soc.,97, 330-339.

Hennington L., R.J.Doviak, D.Sirmans, D. Zrinc, and R.G.Strauch | 1976 | 'Measurements of winds in the optically clear air with microwave pulse-Doppler radar', Preprints 17th Conf. Radar Meteorol. Amer.Meteorol.Soc.,Boston, 342-348.

Hicks J.J. and J.K. Angell | 1968 | 'Radar observations of breaking gravitational waves in the visually clear atmosphere', J.Appl.Meteorol.,7, 114-121.

Hidebrand P.H. | 1976 | 'A Radar Study of Shear Enhanced Turbulent Diffusion', Preprints 17th Conf. on Radar Meteorol., Amer.Meteorol.Soc.,Boston, 330-337.

James, P.K., A.J.Whyman and K.A. Browning | 1978 | 'Radar for clear air measurements', Physics Bulletin, 29,209-210.

Konrad T.G. | 1968 | 'The Alignment of Clear Air Convective Cells', Proc. Intern.Conf. Cloud Physics, Toronto, Canada, 539-543.

Konrad T.G. | 1970 | 'The Dynamics of the Convective Process in Clear Air as seen by Radar', J.Atmos.Sci., 27, 1138-1147.

Konrad T.G. and F.L. Robison | 1972 | 'Simultaneous Measurements of Radar Reflectivity and Refractive index spectra in Clear Air Convection', J.Appl.Meteorol., 11, 1114-1119.

Konrad T.G. and F.L.Robison 1973 'Development and characteristics of free convection in the clear air as seen by radar and aircraft', J.Appl.Meteorol., 12, 1284-1294.

Kropfli R.A. and N.M. Kohn 1976 'Dual Doppler Observations of the convective Mixing Layer at St. Louis' Preprints 17th Conf. on Radar Meteorol., Amer.Meteorol.Soc., Boston, 321-325.

Kropfli R.A., I.Katz, T.G.Konrad and E.B.Dobson 1968 'Simultaneous radar reflectivity measurements and refractive index spectra in the clear atmosphere', Radio Sci., 3,991-994.

Leach W. 1957 'Observed characteristics of convective cell bands', Proc. 6th Weather Radar Conf., Amer.Meteorol.Soc.,Boston, 151-156.

Lee J.T. and R.G.Goff 1976 'Gust Front Wind Shear and turbulence - Concurrent Aircraft and Surface-based Observations', Reprints Seventh Conference on Aerospace and Aeronautical Meteorology and Symposium on Remote Sensing from Satellites. Melbourne, Flo., Amer.Meteorol.Soc., Boston, 48-55.

Lhermitte R.M. 1966 'Probing air motion by Doppler Analysis of Radar Clear Air Returns', J.Atmos.Sci., 23,575-591.

Lhermitte R.M. and D.Atlas 1961 'Precipitation motion by pulse Doppler Radar', Proc. Ninth Weather Radar Conf., Amer.Meteorol.Soc., Boston,218-223.

Ligda M.G.H. and S.G.Bigler 1958 'Radar echoes from a cloudless cold front J.Meteor.,15,494-501.

Luckenback G. 1958 'Two examples of non-precipitating, echoes as observed on AN/CP5-9 radar', Proc. 7th Weather Radar Conf., Amer.Meteorol.Soc., Boston, D41-D47.

Metcalf, J.I. and D.Atlas 1973 'Microscale Ordered Motions and Atmospheric Structure Associated with Thin Echo Layers in stable stratified zones', Boundary-Layer Meteorol., 4, 7-35.

Meyer J.H. 1971 'Radar observations of land breeze fronts', J.Appl.Meteorol.,10,1224-1232.

Miles J.W. and L.N.Howard 1964 'Note on heteorgenous shear flow', J. Fluid Mech., 20,331-336.

Moninger W.R., A.S.Frish, W.C.Campbell and R.G.Strauch | 1978 | 'Doppler radar measurements of plume dispersal and dissipation rates in the Boundary layer', Preprints 18th Conf. on Radar Meteorol., Amer.Meteorol.Soc., Boston, 49-54.

Noonkester V.R. | 1976 | 'The evolution of the clear air convective layer revealed by surface-based sensors', J.Appl.Meteorol., 15, 594-606.

Noonkester V.R. | 1978 | 'Multi Sensor Measurements of Ocean Based Convective Activity', Preprints 18th Conf. on Radar Meteorol. Amer.Meteorol.Soc., Boston, 55-64.

Noonkester V.R. and D.R.Jensen | 1975 | 'The Growth and Decay of the Convective Field revealed by surface based remote sensors', Preprints 16th Radar Meteorol.Conf., Amer.Meteorol.Soc., Boston, 304-311.

Noonkester V.R., D.R.Jensen, J.H.Richter, W.Viezee and R.T.H. Collis | 1974 | 'Concurrent FM-CW radar and lidar observations of the Boundary layer', J.Appl.Meteorol., 13, 249-256.

Noonkester V.R., J.H.Richter, and D.R.Jensen | 1976a | 'Meteorological Interpretation of FM-CW Radar and Acoustic sounder echoes in a coastal environment' Preprint Volume: Conference on Coastal Meteorology Sept 21-23 1976 Virginia Beach, Va., Amer.Meteorol.Soc., Boston, 20-27.

Noonkester V.R., J.H.Richter and D.R. Jensen | 1976b | 'Marine Fog Investigations in San Diego', Preprints 17th Conf. on Radar Meteorol., Amer.Meteorol.Soc., Boston, 282-289.

O'Bannon T. | 1978 | 'A study of Dual-Doppler Synthesized Clear Air Wind Fields', Preprints 18th Conf. on Radar Meteorol., Amer.Meteorol.Soc., Boston, 65-69.

Ochs G.R. and R.S.Lawrence | 1972 | 'Temperature and C_n^2 profiles measured over land and ocean to 3 km above the surface', NOAA Tech. Report ERL 251-WPL22.

Ottersten H. | 1968 | 'Theoretical Aspects on CAT detection by Radar', Preprints 18th Conf. on Radar Meteorol., Amer.Meteorol.Soc., Boston, 252-257.

Ottersten H. | 1969a | 'Atmospheric structure and radar backscattering in clear air', Radio Sci., 4 1179-1193.

Ottersten H. 1969b 'Radar backscattering from the turbulent clear atmosphere', Radio Sci., 4 1251-1255.

Ottersten H., K.R. Hardy and C.G.Little 1973 'Radar and Sodar probing of waves and turbulence in statically stable clear-air layers', Boundary Layer Meteorol., 4, 47-89

Readings C.J., E. Golton and K.A.Browning 1973 'Fine Scale Structure and Mixing within an Inversion', Boundary-Layer Meteorol., 4 275-287.

Richter J.H. 1969 'High resolution tropospheric radar sounding', Radio Sci., 4, 1261-1268.

Richter J.H., D.R.Jensen, Pappert R.A. andV.R. Noonkester, 1973a 'New developments in FM-CW radar sounding Boundary-layer Meteorol., 4, 179-199.

Richter J.H., D.R. Jensen, V.R.Noonkester, J.B. Kreasky, M.W. Stillmann and W.N.Wolf 1973b 'Remote Radar Sensing', Atmospheric Structure and Insects', Science, 180, 1176-1178.

Richter J.H., D.R. Jensen, V.R.Noonkester, T.G.Konrad, A.Arnold and J.R.Rowland 1974 'Clear Air Convection: a close look at its evolution and structure' Geophys.Res. Letters 1 173-176.

Riley J.R. 1979 'Radar as an aid to the study of insect flight', in A Handbook on Biotelemetry and Radio Tracking, edited by C.J. Amlaner Jr. and D.W. Macdonald, pp131-141, Pergamon Press, Oxford.

Röttger J. 1978 'Evidence for partial reflection of VHF radar signals from the troposphere', J.Geophys., 44, 393-394.

Röttger J. 1979 'VHF Radar Observations of a Frontal Passage', J.Appl. Meteorol., 18, 85-91

Röttger J. and C.H. Liu 1978 'Partial reflection and scattering of VHF radar signals from the clear atmosphere', Geophys.Res. Lett., 5, 357-360.

Röttger J. and G. Schmidt 1979 'High Resolution VHF Radar Sounding of the Troposphere and Stratosphere. to be published in IEE Trans.Geosci. Electr.

Röttger J. and R.A. Vincent 1978 'UHF radar studies of tropospheric velocities and irregularities using spaced antenna techniques', Geophys.Res. Lett., 5, 917-920.

Röttger J., J.Klostermeyer, P.Czechowsky, R.Rüster and G. Schmidt	1978	'Remote sensing of the Atmosphere by VHF Radar Experiments', Naturwissenschaften, 65, 285-296.
Rowland J.R.	1973	'Intensive Probing of a Clear Air Convective Field by Radar and Instrumented Drone Aircraft', J.Appl.Meteorol., 12 149-155.
Rowland J.R. and A. Arnold	1975	'Vertical velocity structure and geometry of Clear Air Convective Elements Preprints of 16th Radar Meteorol.Conf., Amer.Meteorol.Soc., Boston, 296-303.
Simpson J.E., D.A.Mansfield and J.R.Milford	1977	'Inland penetration of sea-breeze fronts', Quart. J.Roy.Meteorol.Soc., 103 47-76.
Sirmans D. and B. Bumgarner	1975	'Numerical comparison of five mean frequency estimators', J.Appl.Meteorol., 14, 991-1003.
Starr J.R. and K.A. Browning	1972	'Observations of lee waves by High-Power Radar', Quart. J.Roy.Met. Soc., 98, 73-85.
Strauch R.G.	1976	'Theory and Application of the FM-CW Doppler Radar', Ph.D. Thesis, University of Colorado.
Strauch R.G. and R.B.Chadwick	1976	'Measurement capabilities of FM-CW Doppler radars', Preprints 17th Conf. on Radar Meteorol., Amer.Meteorol.Soc., Boston, 29-32.
Strauch R.G. and W.R. Moninger	1978	'Radar Measurement of Wind Shear and Wind profiles for air safety', Preprints 18th Conf. on Radar Meteorol., Amer.Meteorol.Soc., Boston, 432-436.
Tatarski V.I.	1961	'Wave Propagation in a Turbulent Medium', 285pp., McGraw Hill Book Co.Inc.New York.
VanZandt T.E., J.L. Green, J.M.Warnock and R.H.Winkler	1975	'Studies of Winds in the Upper troposphere with a sensitive VHF radar', Preprints 16th Radar Meteorol. Conf. Amer.Meteorol.Soc., Boston, 316-319.
VanZandt T.E., J.L. Green, K.S.Gage and W.L. Clark	1978	'Vertical profiles of refractivity turbulence structure constant: Comparison of observations by the Sunset Radar with a new theoretical model', Radio Sci., 13 819-829.
VanZandt T.E., J.L. Green and W.L.Clark	1979	'Bouyancy waves in the troposphere: Doppler radar observations and a theoretical model', Geophys. Res. Lett., 6, 429-432.

Watkins C.D. and K.A. Browning 1973 'The detection of clear air turbulence by radar', Physics in Technology 4, 28-61, published by the Institute of Physics, London.

TABLE 1

RADAR	WAVELENGTH (cm)	BEAMWIDTH (deg)	ANTENNA DIMENSIONS (m)	RANGE RESOLUTION (m)	PEAK POWER (MW)	MINIMUM DETECTABLE C_n^2 AT ($m^{-2/3}$)	RANGE (Km)	ANTENNA CONFIGURATION
						NOTE: SEE	TABLE CAPTION	
FM-CW, SAN DIEGO	10	2.3	3 diam	1	150 watts	5×10^{-13}	1	twin dish, vertical
FM-CW, COLORADO	10	2.8	2.6 diam	32	200 watts	5×10^{-17}	1	twin dish, steerable
WALLOPS ISLAND	3.2	0.2	10.4 diam	300	0.75	5×10^{-15}	10	steerable dish
NORMAN, OKLAHOMA	10.5	0.8	9.2 diam	180	0.75	3×10^{-16}	10	steerable dish
DEFFORD, ENGLAND	10.7	0.3	25 diam	30	0.3	3×10^{-16}	10	steerable dish
WALLOPS ISLAND	10.7	0.5	18.4 diam	200	3.0	5×10^{-16}	10	steerable dish
CHATANIKA, ALASKA	23	0.6	27 diam	1500	3.0	1×10^{-20}	10	steerable dish
WALLOPS ISLAND	71.5	2.9	18.4 diam	150	6.0	1×10^{-16}	10	steerable dish
SOUSY, GERMANY	561	5	62 diam	50	0.6	1×10^{-19}	10	phased yagi array
POKERFLAT, ALASKA	600	2 x 4	100 x 50	750	0.015	5×10^{-18}	10	phased dipole array
SUNSET, COLORADO	741	5 x 9	60 x 30	1000	0.125	3×10^{-18}	10	phased dipole array

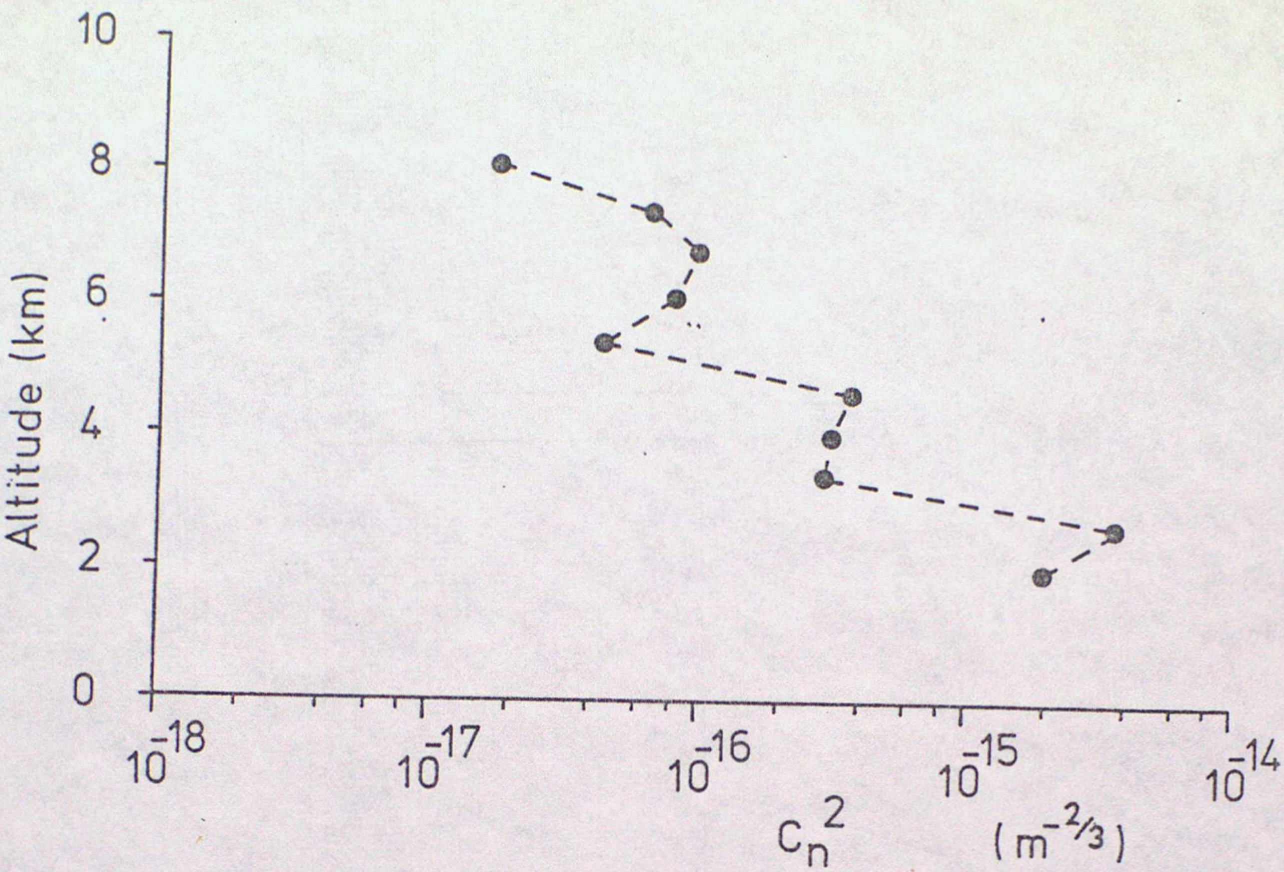

Altitude (km)
10
8
6
4
2
0
10^{-18}
10^{-17}
10^{-16}
10^{-15}
10^{-14}
C_n^2 $(m^{-2/3})$

Fig 1

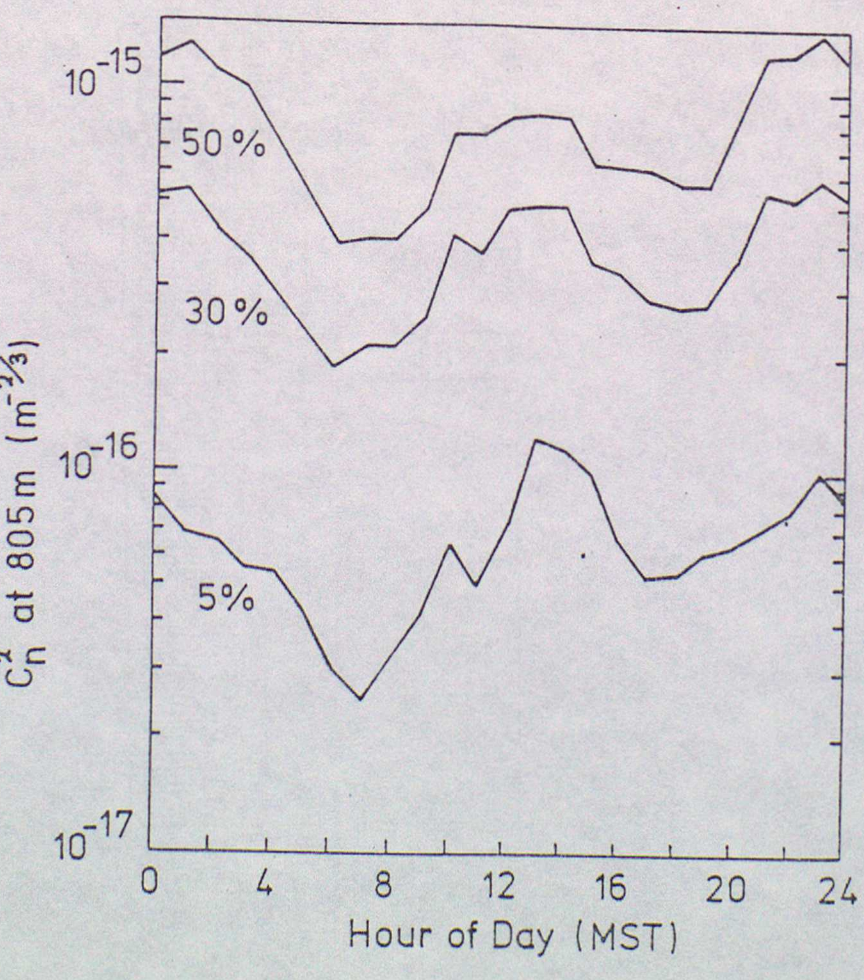

10^{-15}
10^{-16}
10^{-17}
50 %
30 %
5%
C_n^2 at 805 m $(m^{-2/3})$
0
4
8
12
16
20
24
Hour of Day (MST)

Fig 2

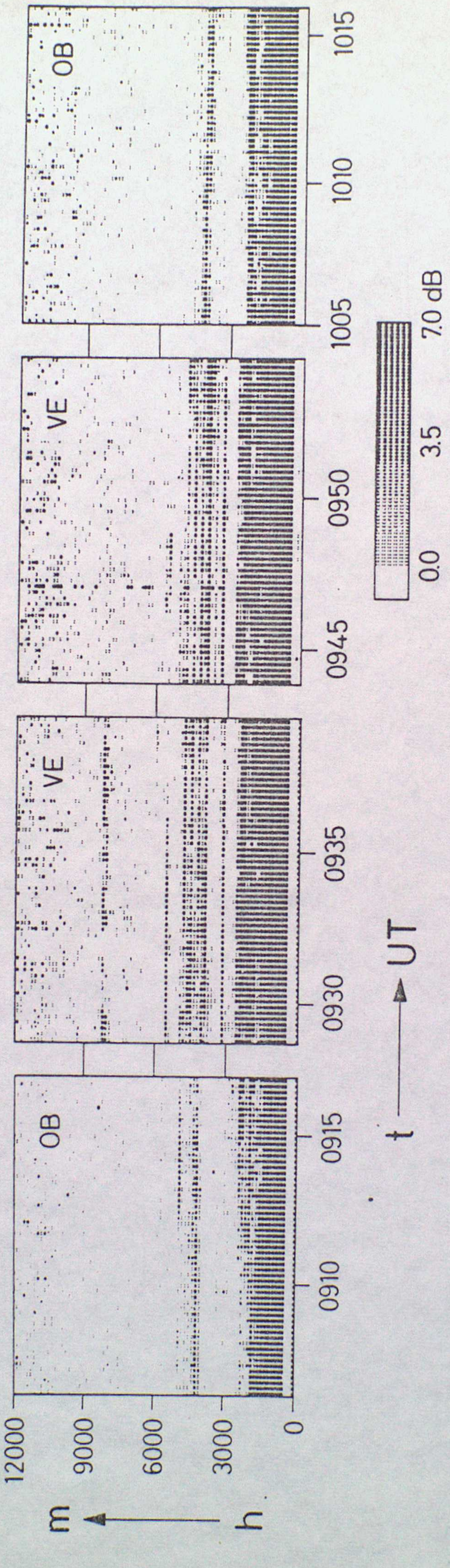
16. 8. 1977
OB
VE
VE
OB
h
m
12000
9000
6000
3000
0
0910
0915
0930
0935
0945
0950
1005
1010
1015
t
UT
0.0
3.5
7.0 dB

Fig 3

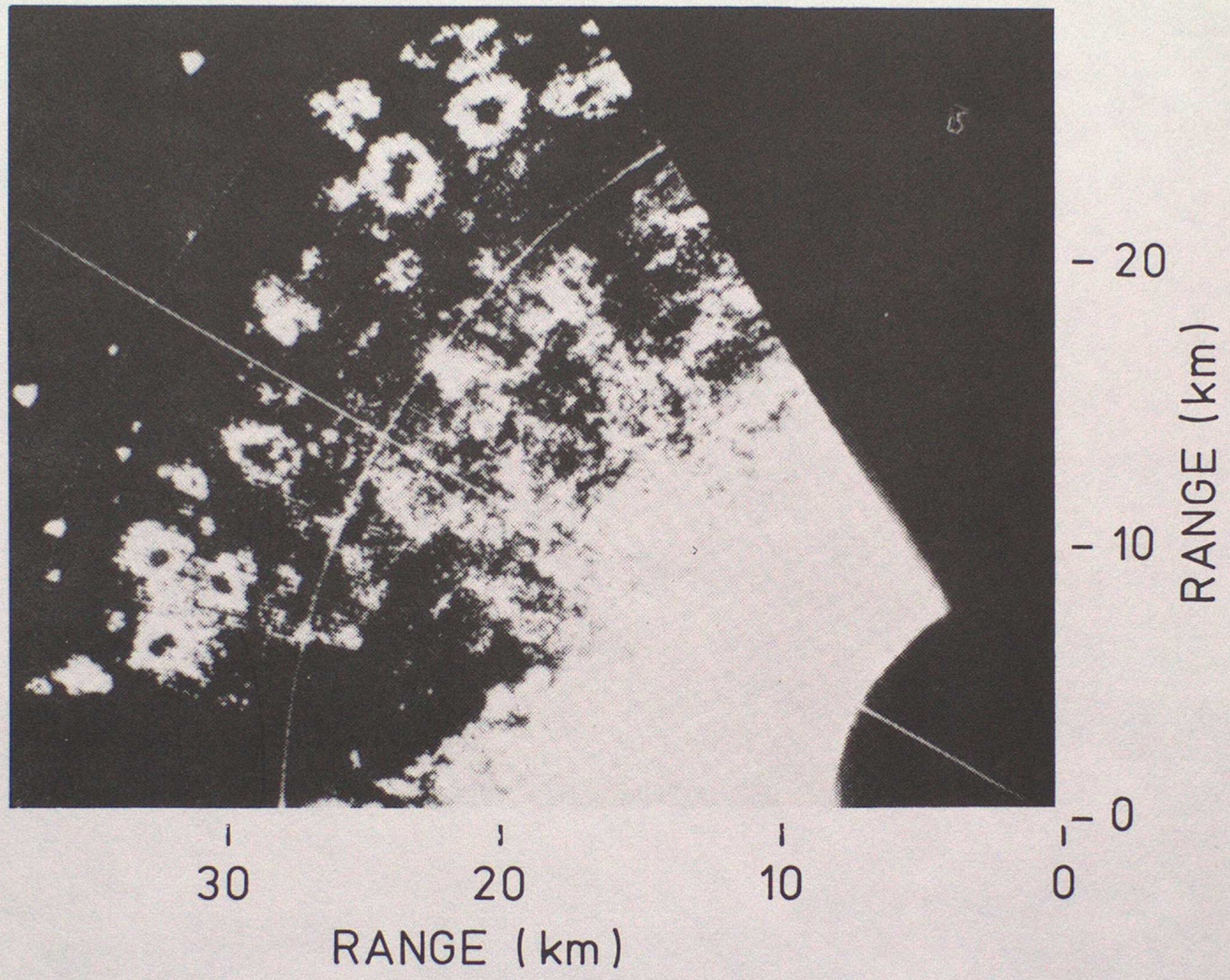

Fig 4

AIRCRAFT AT 450 METERS ALTITUDE

OCTOBER 4, 1973
1041 EST

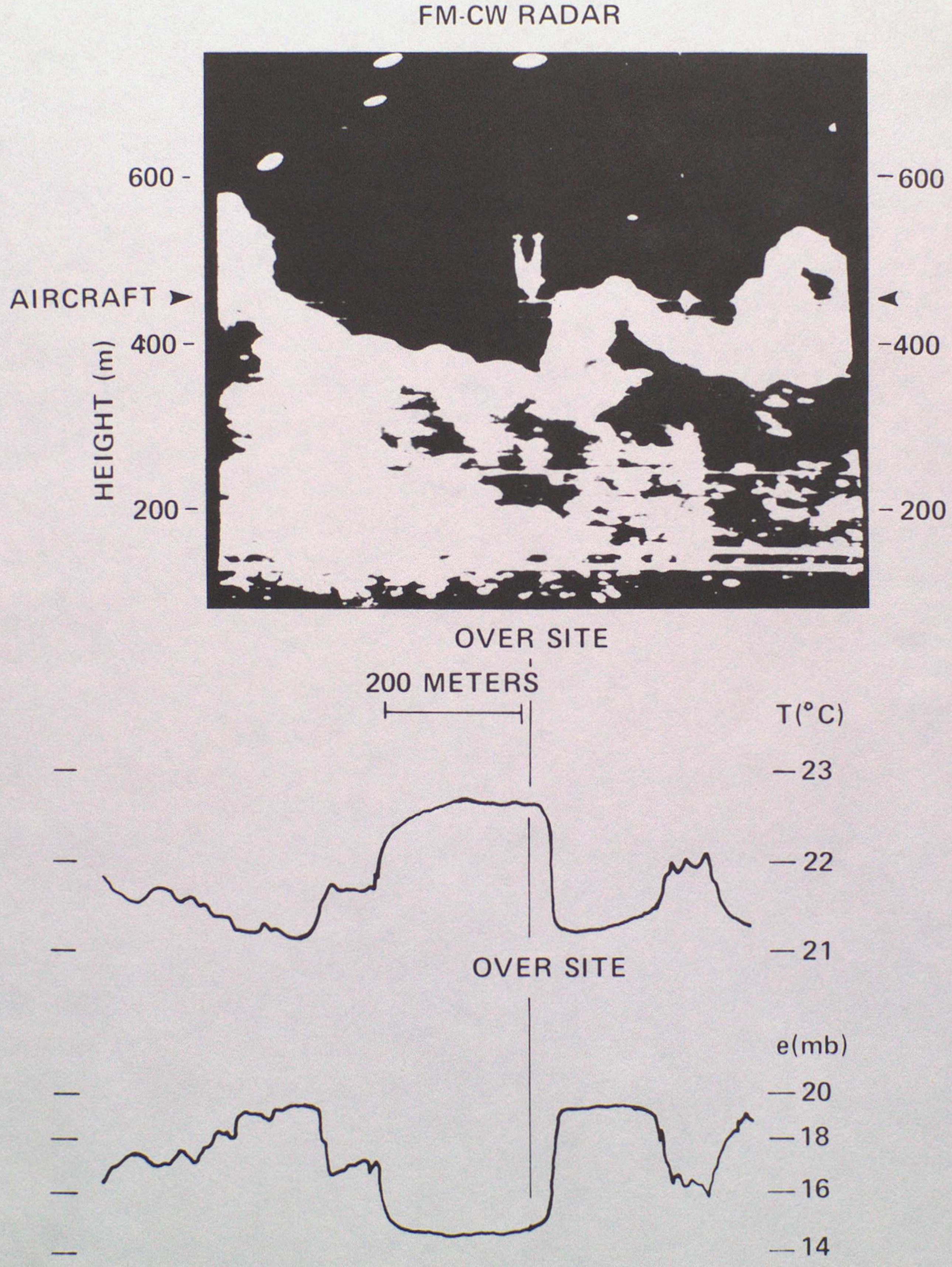

Fig 5

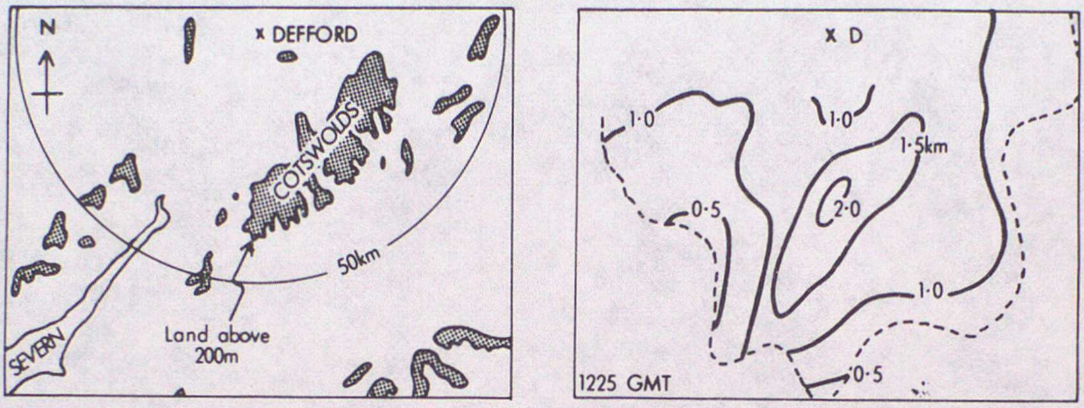
N
x DEFFORD
COTSWOLDS
50km
Land above
200m
SEVERN
X D
1·0
1·0
1·5km
2·0
0·5
1·0
0·5
1225 GMT

FIG 6

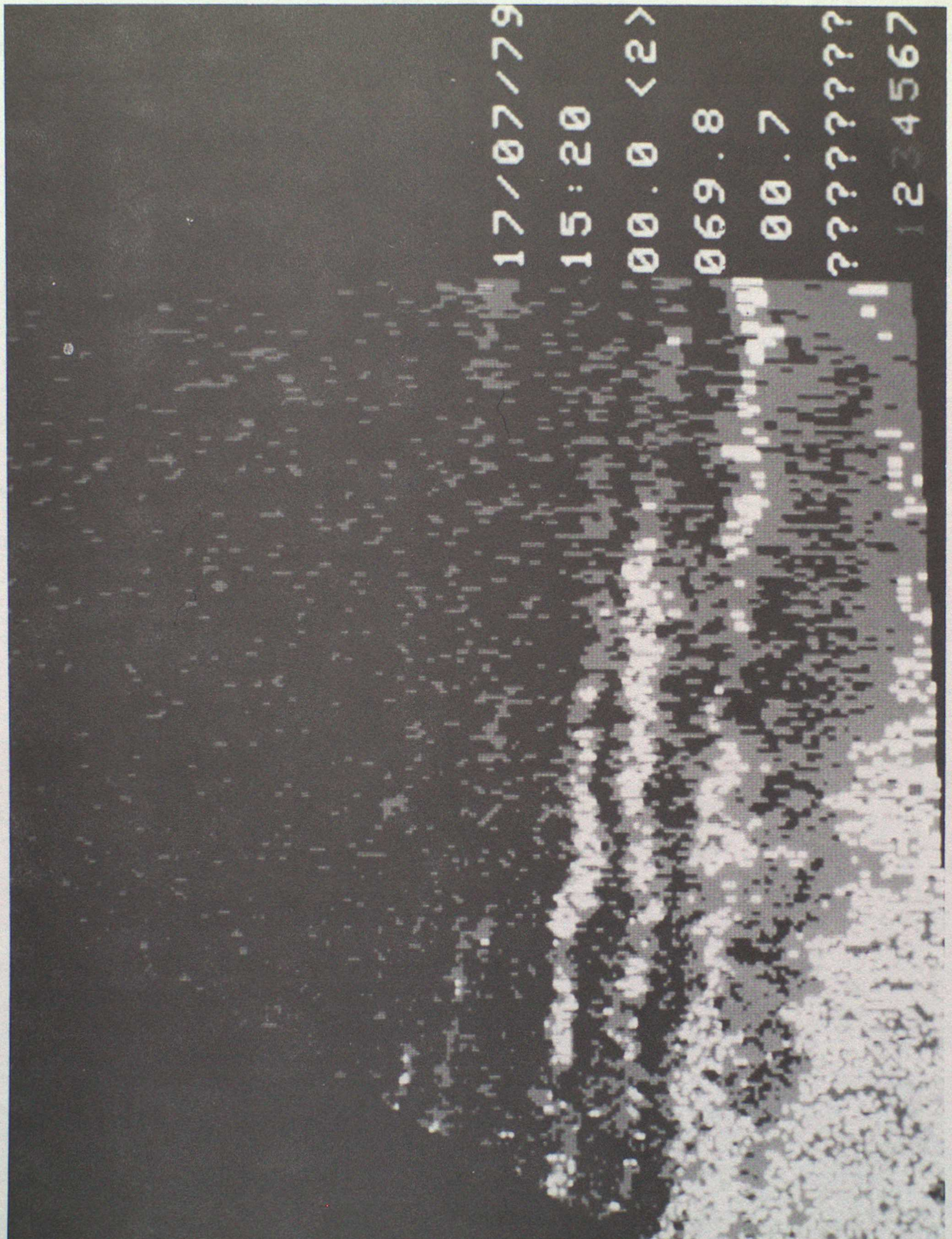

Fig 7

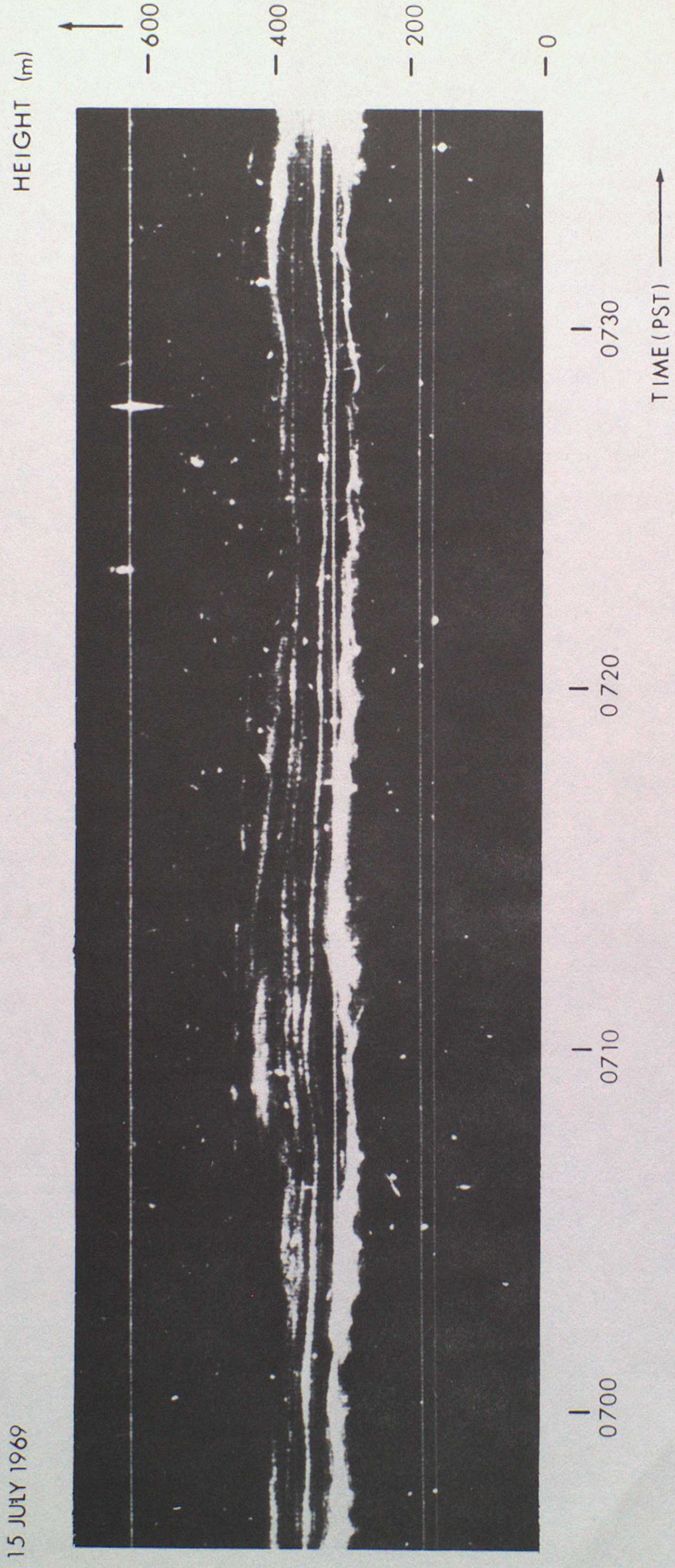

15 JULY 1969
HEIGHT (m)
600
400
200
0
0700
0710
0720
0730
TIME (PST)

Fig 8

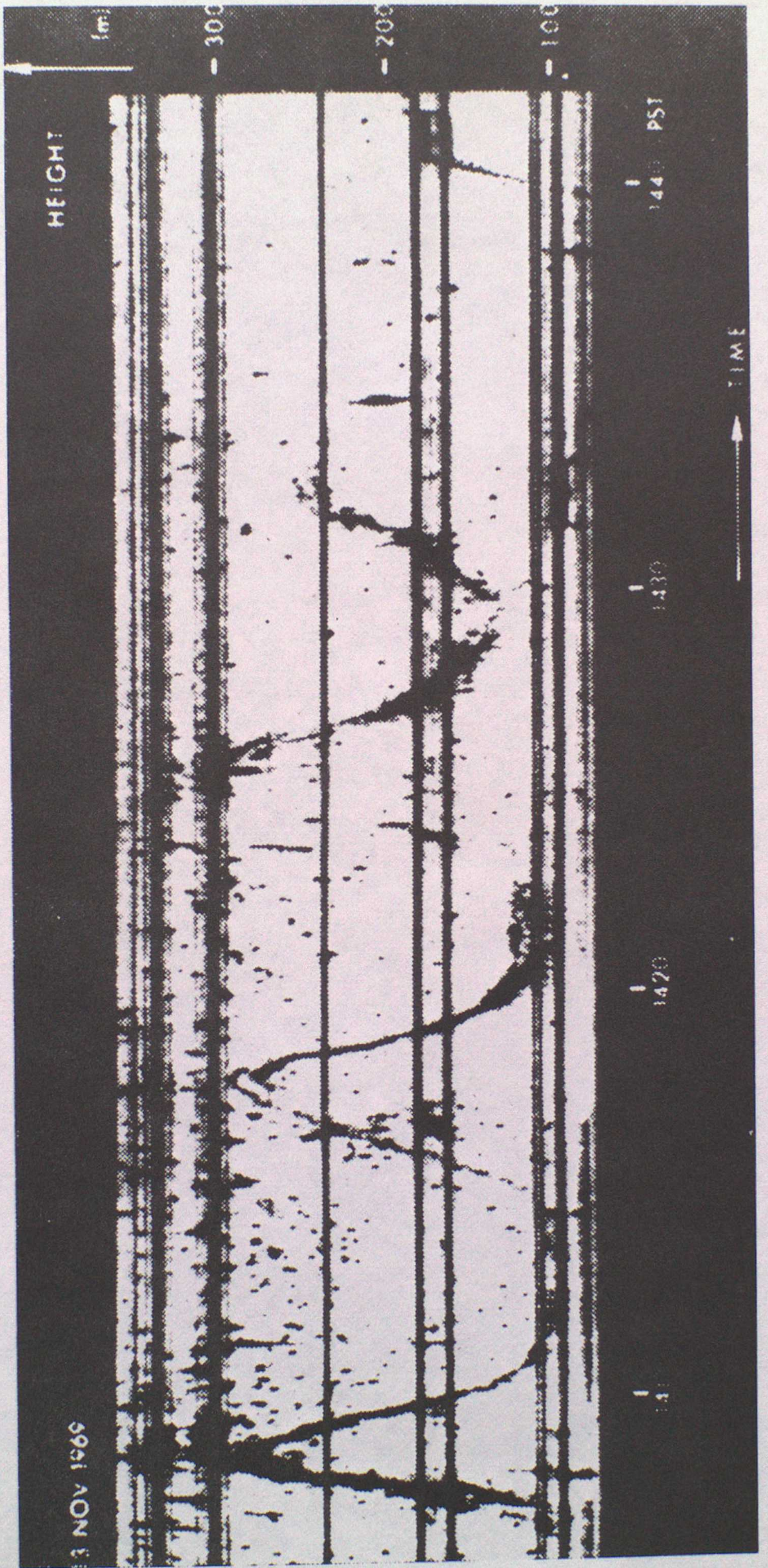

Fig 9

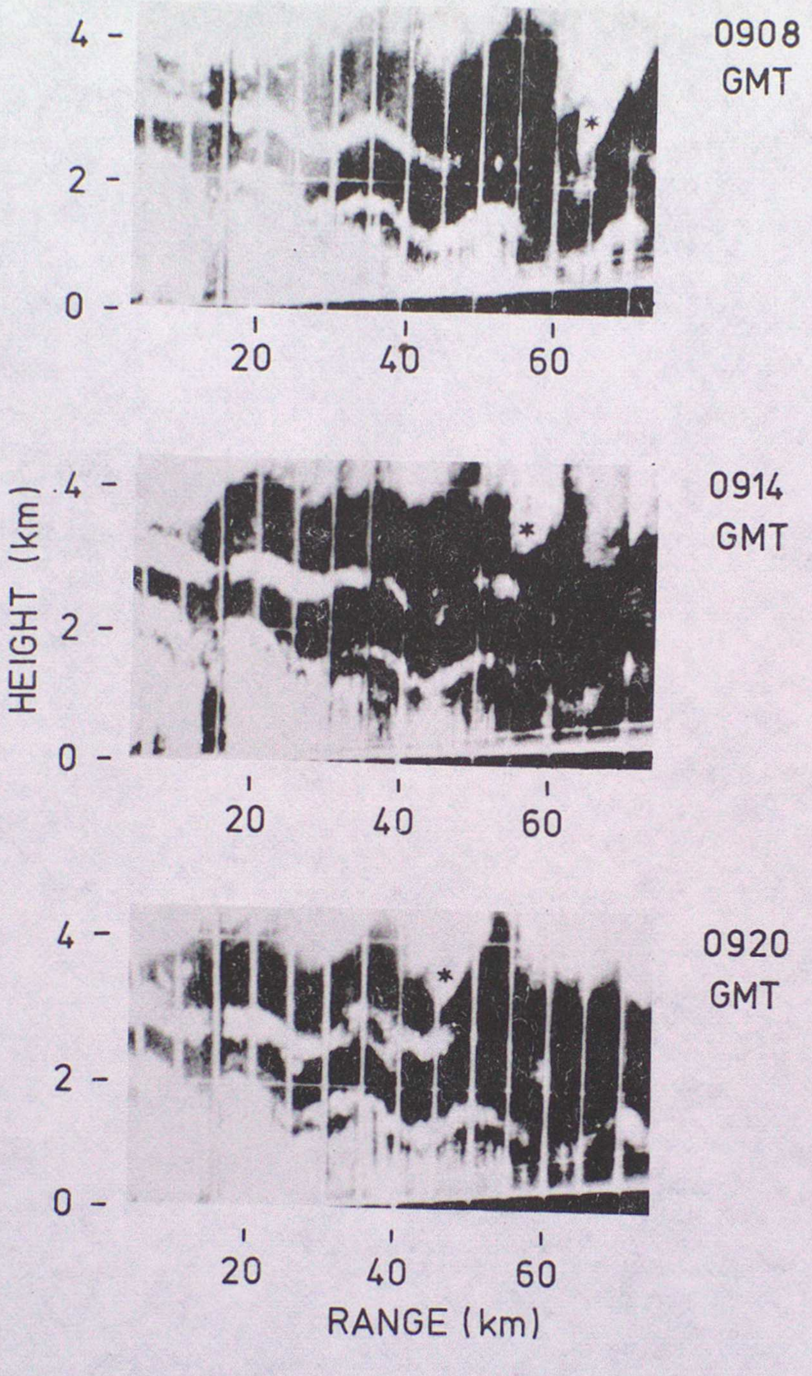
4
2
0
20
40
60
0908
GMT
*
HEIGHT (km)
4
2
0
20
40
60
0914
GMT
*
4
2
0
20
40
60
0920
GMT
*
RANGE (km)

FIG 10

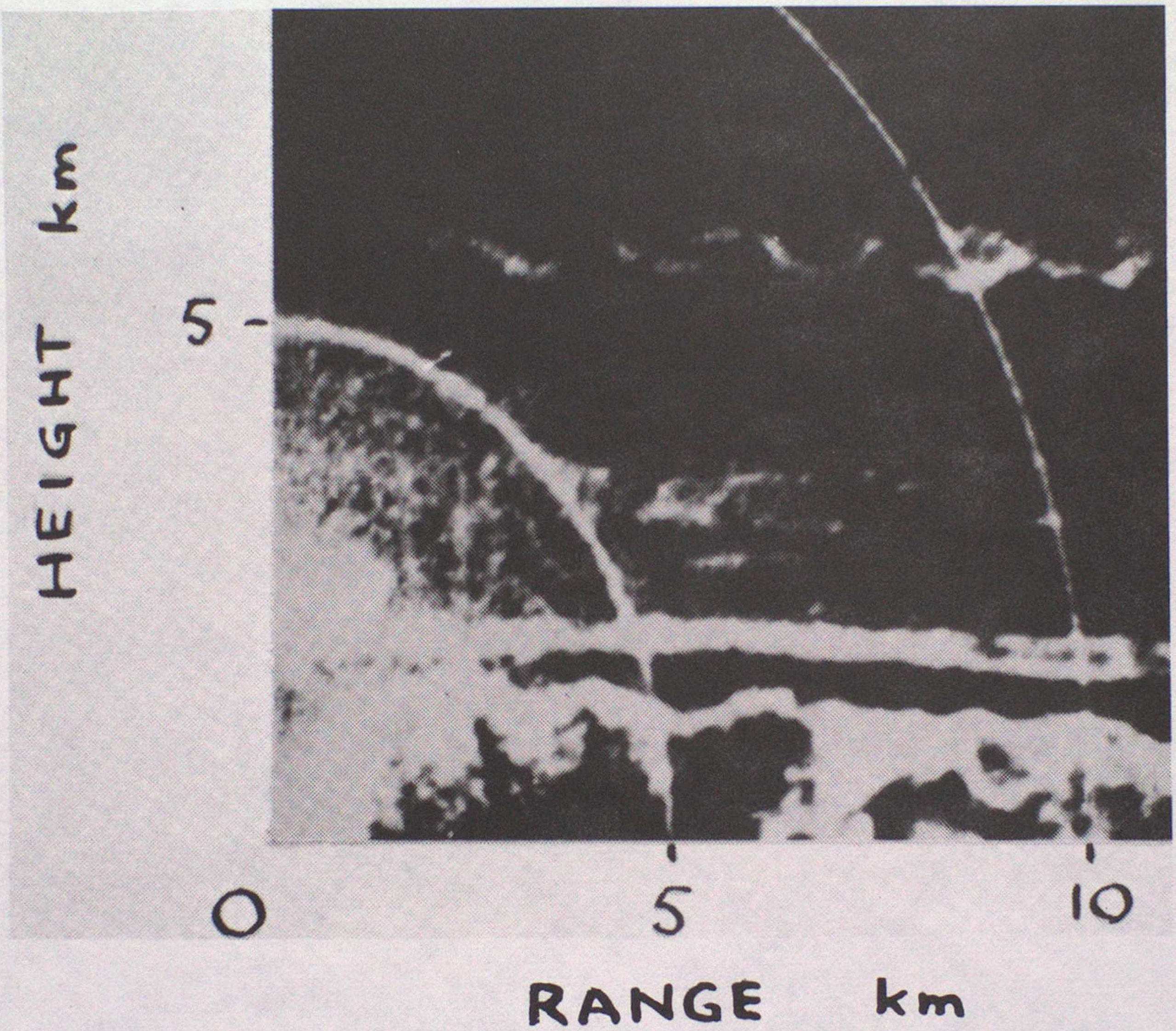

Fig 11

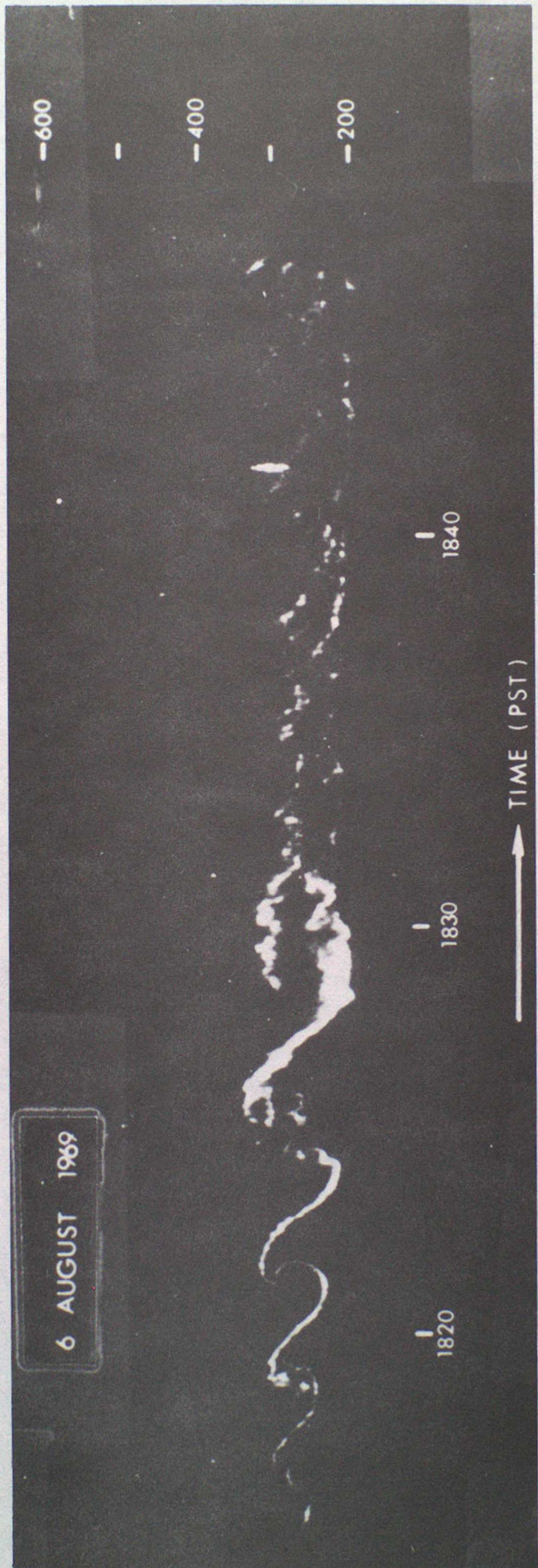

Fig 12

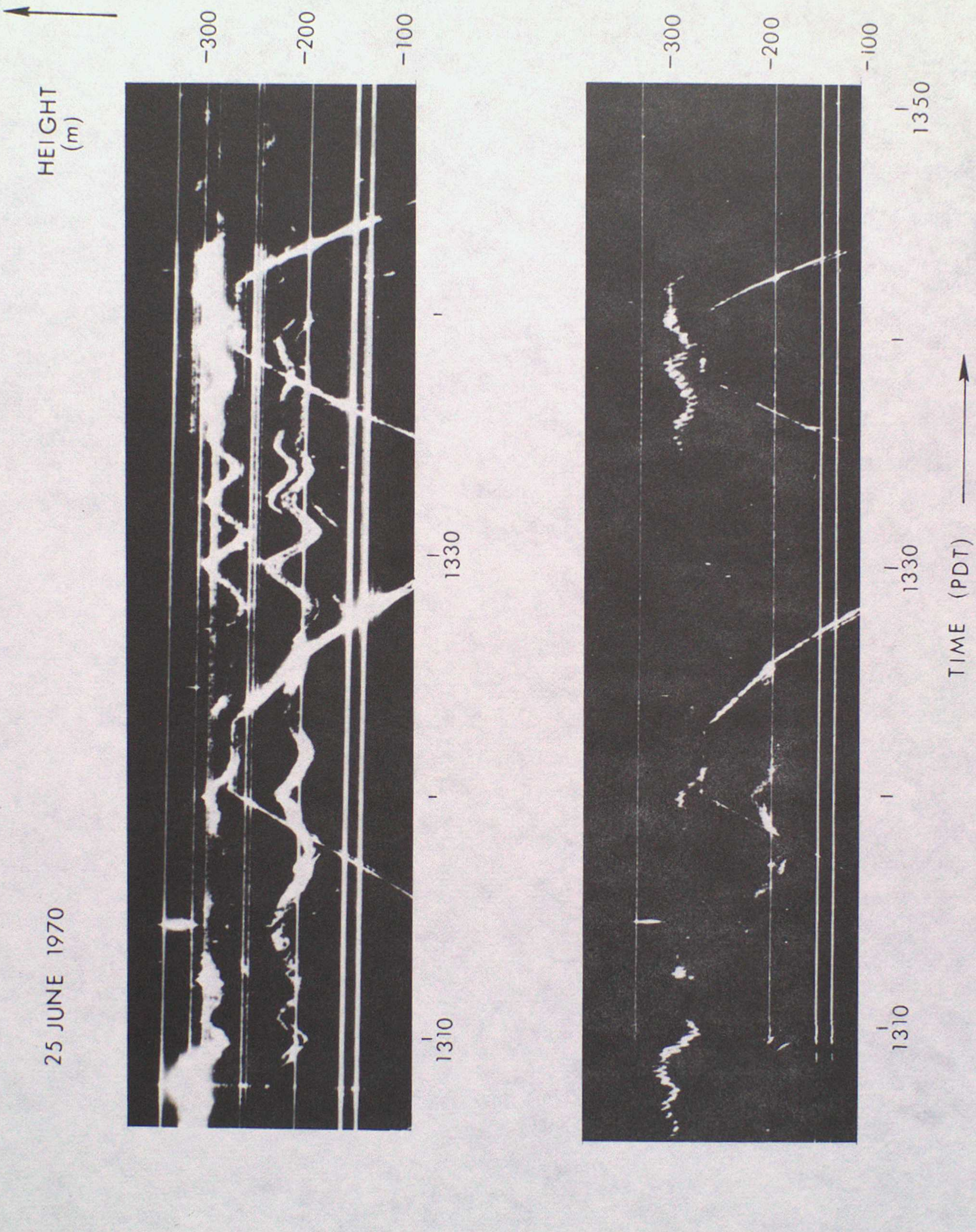

Fig 13

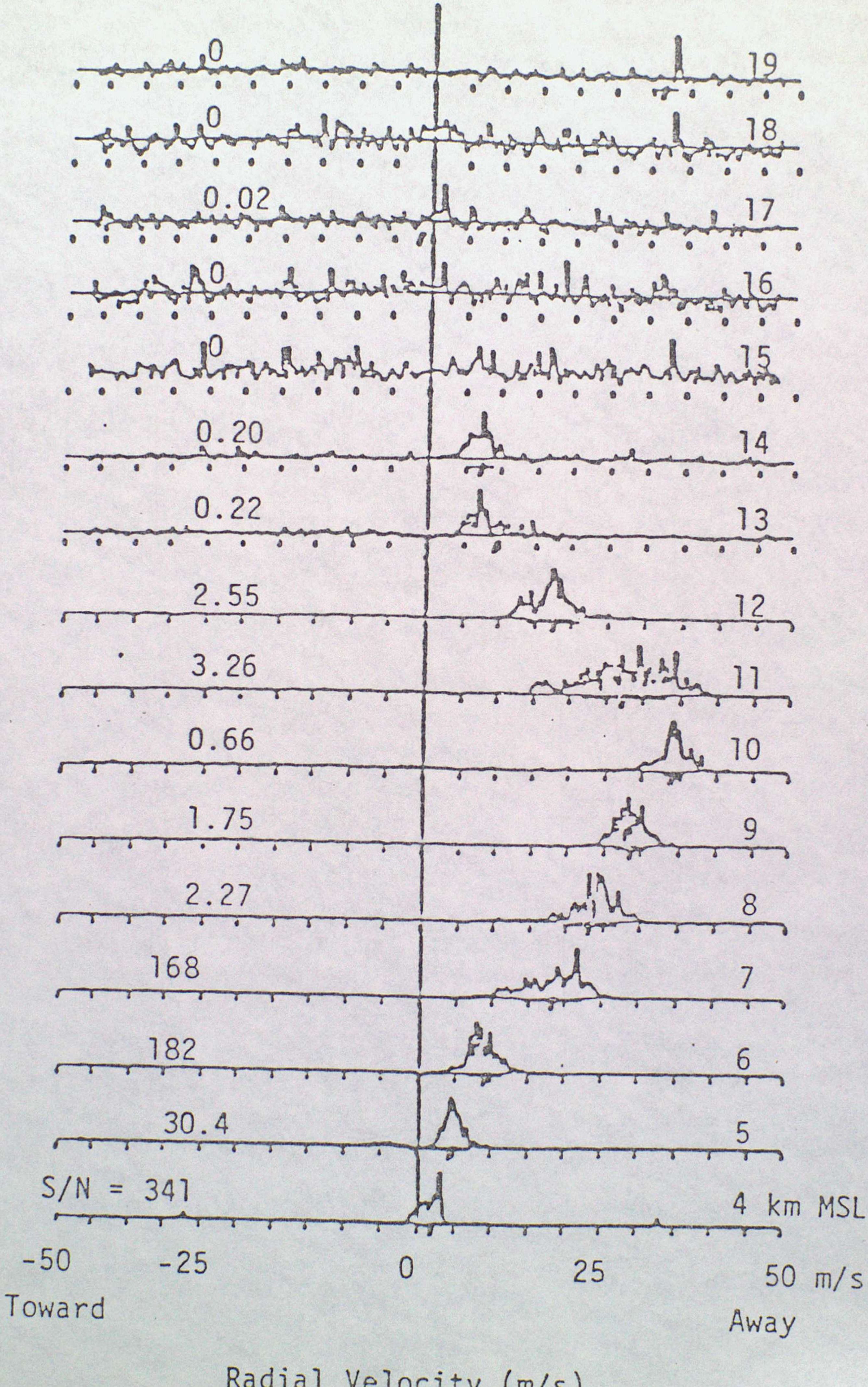
0
19
0
18
0.02
17
0
16
0
15
0.20
14
0.22
13
2.55
12
3.26
11
0.66
10
1.75
9
2.27
8
168
7
182
6
30.4
5
S/N = 341
4 km MSL
-50
-25
0
25
50 m/s
Toward
Away
Radial Velocity (m/s)

Fig 14

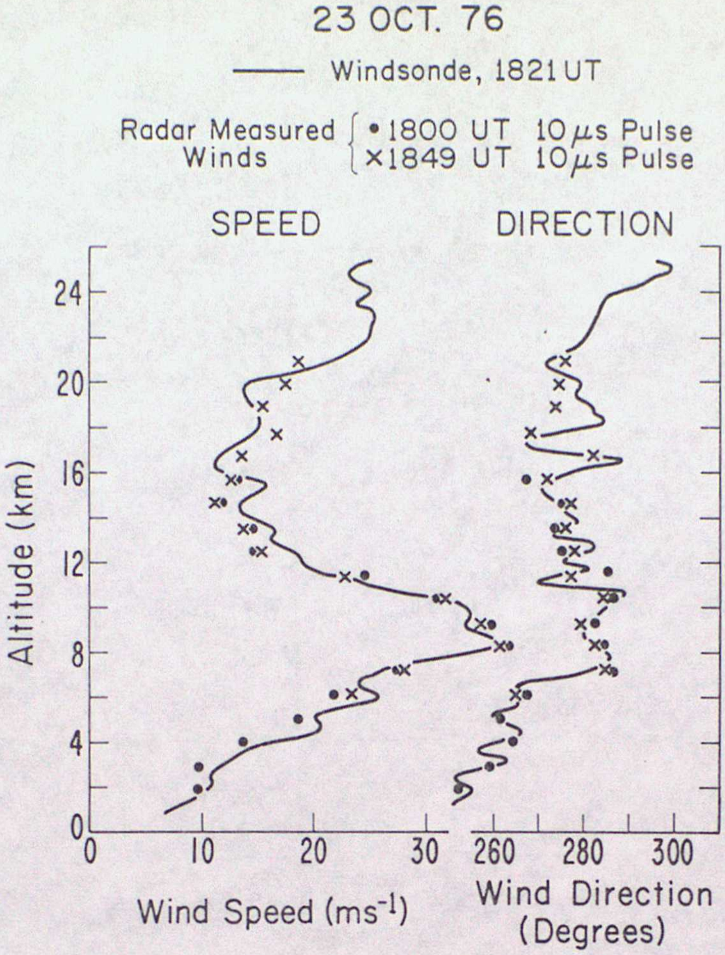
23 OCT. 76
Windsonde, 1821 UT
Radar Measured Winds
• 1800 UT 10 μs Pulse
× 1849 UT 10 μs Pulse
SPEED
DIRECTION
Altitude (km)
0
4
8
12
16
20
24
0
10
20
30
260
280
300
Wind Speed (ms-1)
Wind Direction (Degrees)

Fig 15

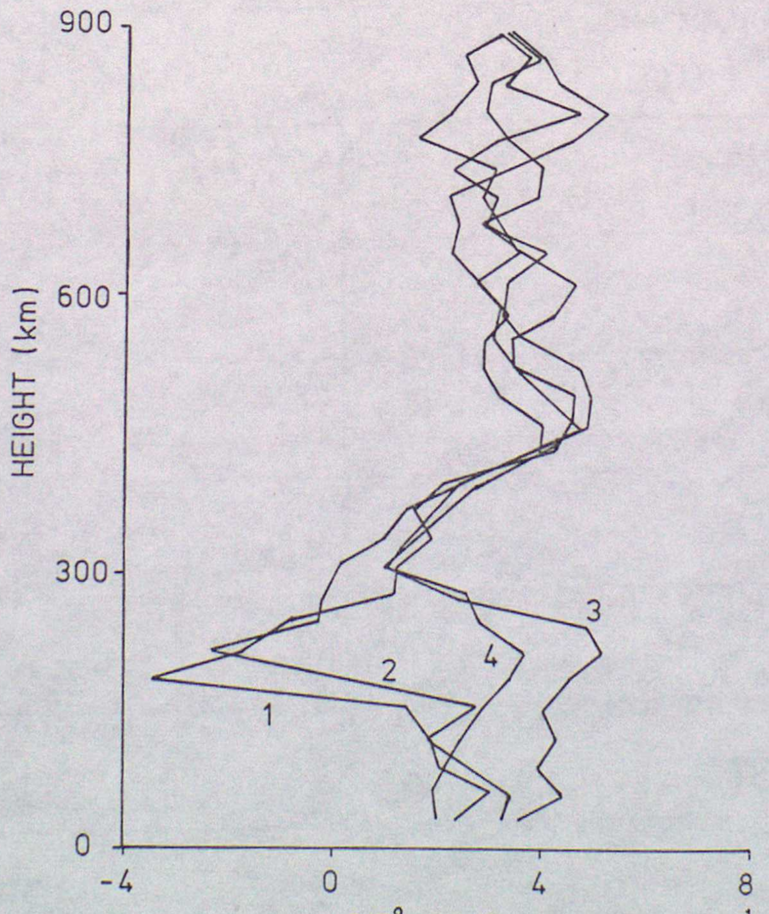
HEIGHT (km)
0
300
600
900
1
2
3
4
-4
0
4
8
315° WIND VELOCITY (ms-1)

Fig 16

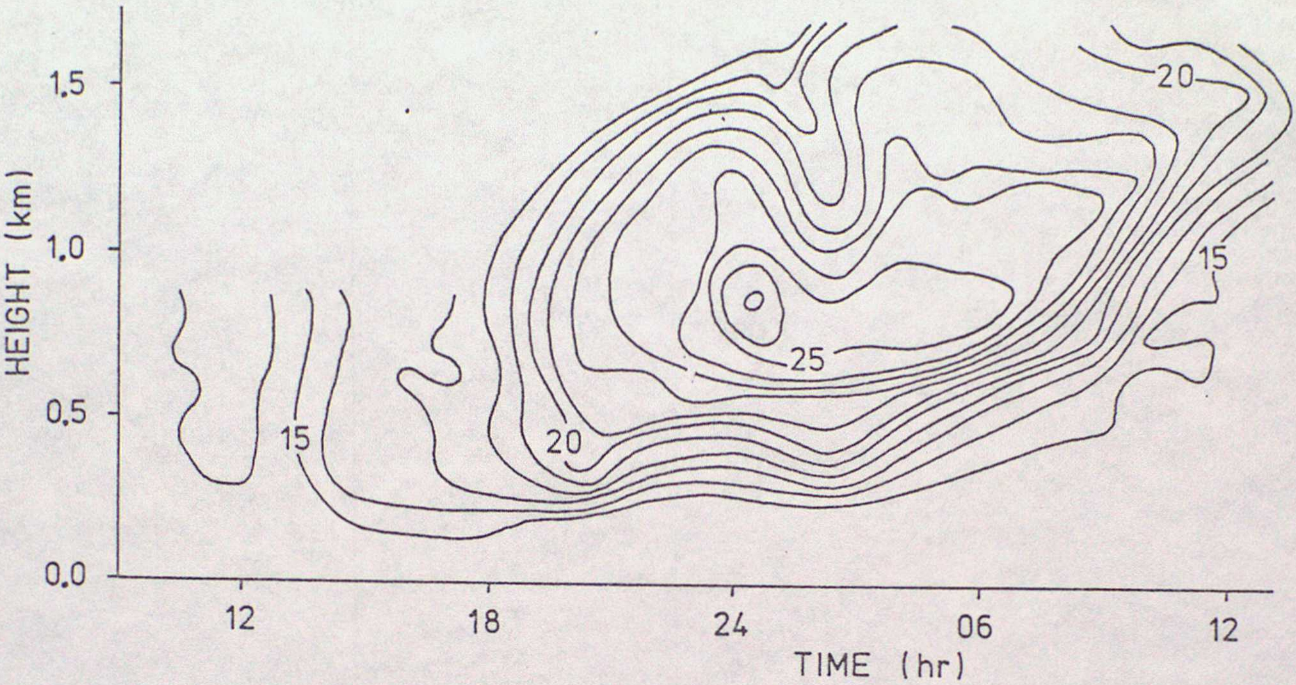
HEIGHT (km)
1.5
1.0
0.5
0.0
15
20
25
0
20
15
12
18
24
06
12
TIME (hr)

Fig 17

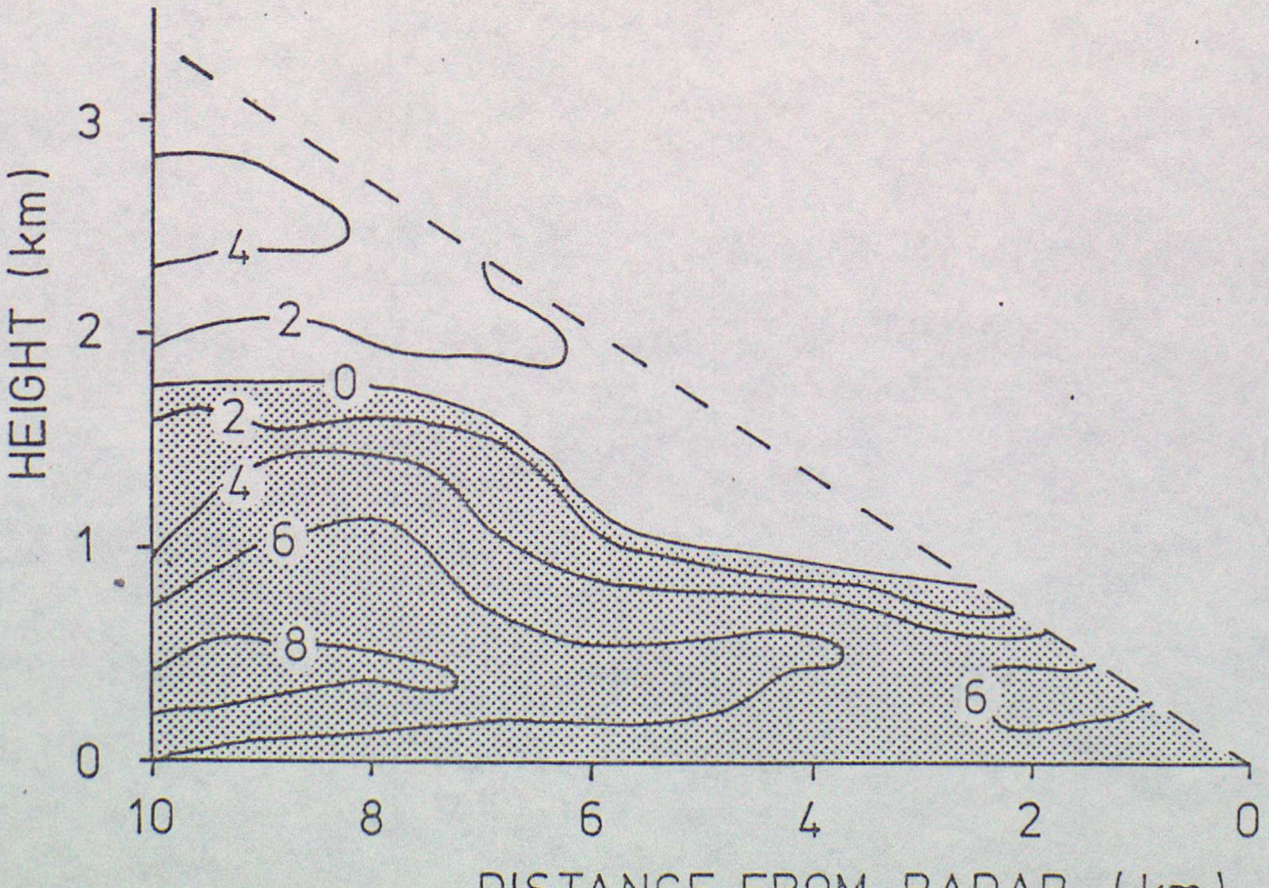
HEIGHT (km)
3
2
1
0
4
2
0
2
4
6
8
6
10
8
6
4
2
0
DISTANCE FROM RADAR (km)

Fig 18

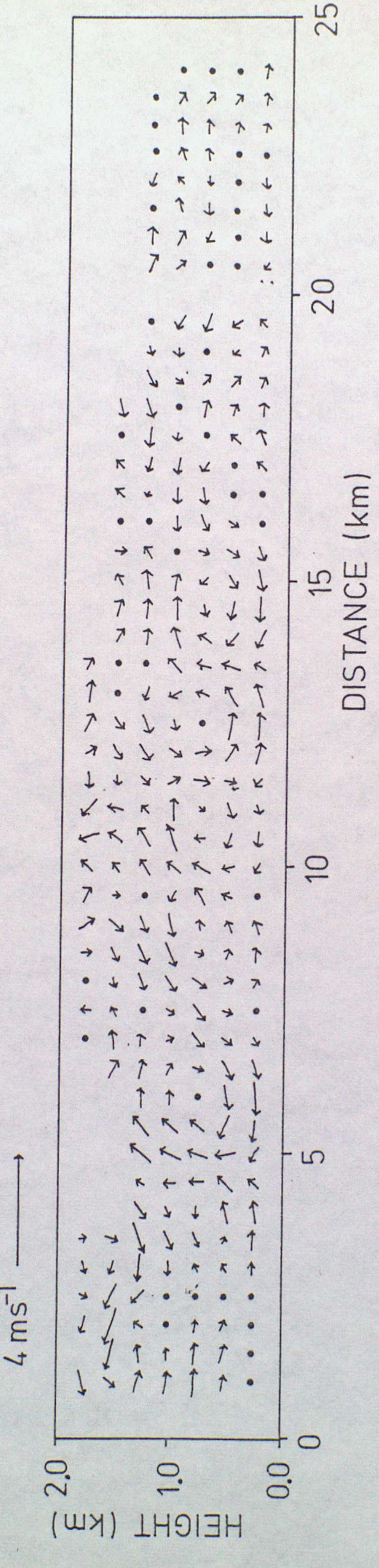

Fig 19

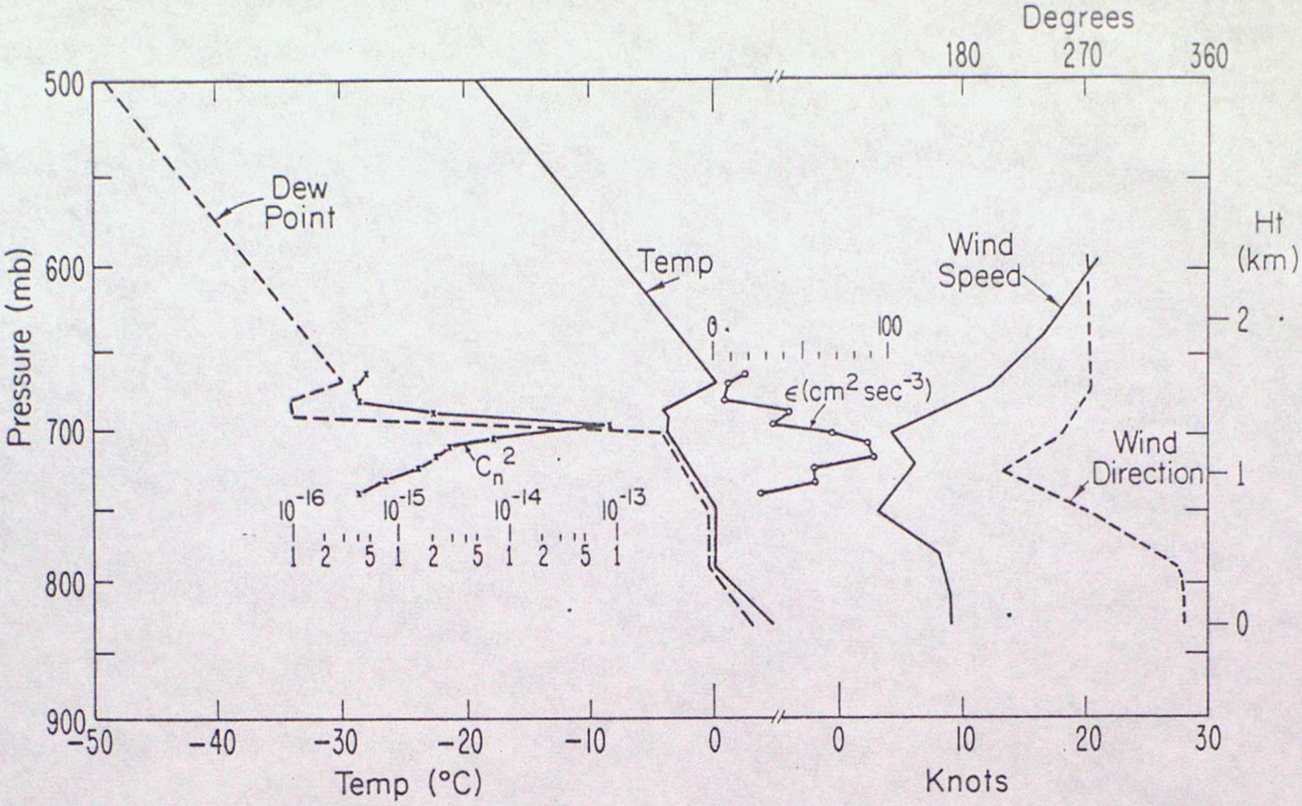
Degrees
180
270
360
500
600
700
800
900
Pressure (mb)
Dew Point
Temp
Wind Speed
Ht (km)
2
1
0
0
100
ϵ (cm^2 sec^{-3})
$C_n^{\,2}$
Wind Direction
10^{-16}
10^{-15}
10^{-14}
10^{-13}
1 2 5 1 2 5 1 2 5 1
−50 −40 −30 −20 −10 0
0 10 20 30
Temp (°C)
Knots

Fig 20

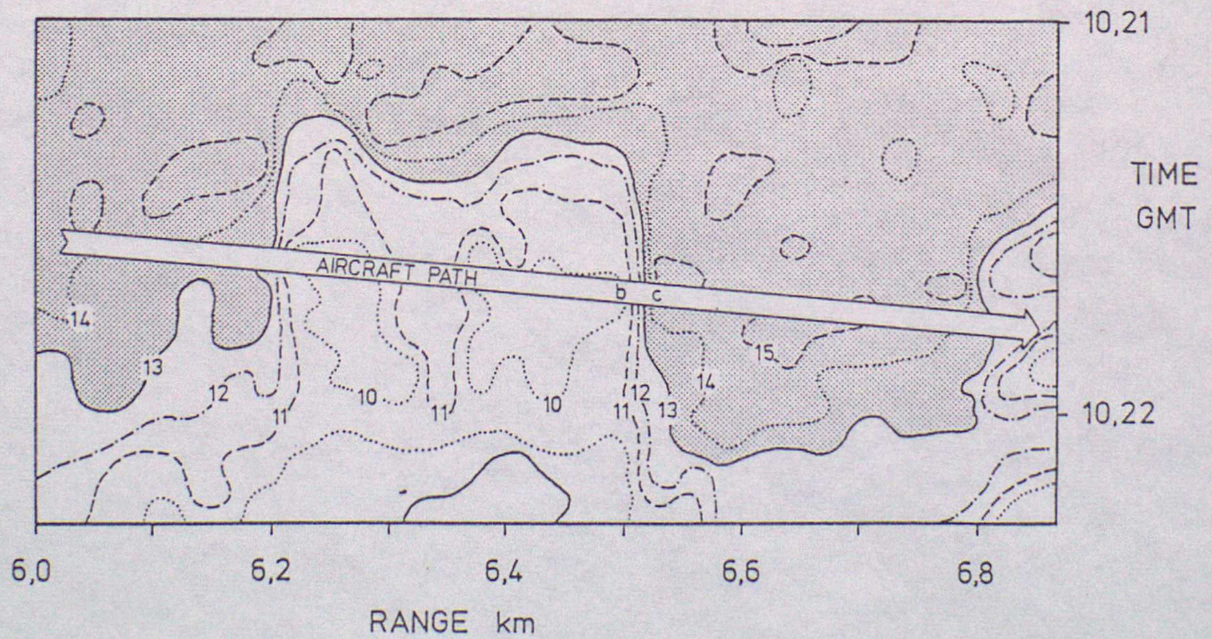
AIRCRAFT PATH
b c
14
13
12
11
10
11
10
11
12
13
14
15
10,21
10,22
TIME GMT
6,0 6,2 6,4 6,6 6,8
RANGE km

Fig 21

METEOROLOGICAL OFFICE RADAR RESEARCH LABORATORY - MET O RRL

Research Reports

No 1 The Short Period Weather Forecasting Pilot Project
K A Browning

No 2 Observation of Strong Wind Shear using Pulse Compression Radar.
K A Browning, P K James (Met O RRL). D M Parkes, C Rowley A J Whyman (RSRE)

No 3 Assessment of a Real-Time Method for Reducing the Errors in Radar Rainfall Measurements due to Bright-Band
J L Clarke, RSRE, C G Collier, Met O RRL

No 4 Meteorological Applications of Radar
K A Browning

No 5 Structure of the Lower Atmosphere Associated with Heavy Falls of Orographic Rain in South Wales.
J Nash, K A Browning

No 6 On the Benefits of Improved Short Period Forecasts of Precipitation to the United Kingdom - Non Military Applications Only
C G Collier

No 7 Persistence and Orographic Modulation of Mesoscale Precipitation Areas in a Potentially Unstable Warm Sector.
F F Hill, K A Browning

No 8 Mesoscale Structure of Line Convection at Surface Cold Fronts.
P K James, K A Browning

No 9 Objective Forecasting Using Radar Data: A Review
C G Collier

No 10 Structure, Mechanism and Prediction of Orographically Enhanced Rain in Britain: A Review
K A Browning

No 11 A Strategy for Using Radar & Satellite Imagery for Very-Short-Range Precipitation Forecasting.
K A Browning, C G Collier, P Menmuir.

75